A genetic signature of resistance to activity-based anorexia in striatal projecting cortical neurons.

Huang K[1,2], Magateshvaren Saras MA[3,4], Conn K[1,2], Greaves E[1,2], Reed F[1,2,5], Tyagi S[4,6], Munguba H[7] & Foldi CJ[1,2]*

[1] Monash University, Department of Physiology, 26 Innovation Walk, Clayton VIC 3800

[2] Monash Biomedicine Discovery Institute, 23 Innovation Walk, Clayton VIC 3800

[3] IITB-Monash Research Academy, Mumbai, Maharashtra, 400076, India

[4] Monash University, Central Clinical School, 99 Commercial Road, Melbourne VIC 3004

[5] Australian Eating Disorders Research and Translation Centre, University of Sydney, NSW 2006

[6] RMIT, School of Computing Technologies, 124 La Trobe Street, Melbourne VIC 3001

[7] Department of Neuroscience, Physiology & Pharmacology, University College London, WC1E 6BT, UK

***Correspondence**: Dr Claire Foldi; email: claire.foldi@monash.edu, Department of Physiology, Monash University, 26 Innovation Walk, Clayton VIC 3800 Australia

Funding: This work was supported by a National Health and Medical Research Council (NHMRC) of Australia Ideas Grant (GNT2001722) awarded to CJF. K.H. is supported by a Monash Graduate Scholarship (MGS) and K.C. is supported by a Monash Faculty Early Career Postdoctoral Fellowship.

Disclosures: None

Word count: 5232

Abstract

Anorexia nervosa (AN) is a complex psychiatric disorder characterised by severe pathological weight loss and persistent cognitive inflexibility. Converging evidence from neuroimaging studies and genome-wide association study (GWAS) suggests the involvement of prefrontal cortex (PFC) and striatum dysfunction in the pathophysiology of AN. However, identifying the causal role of circuit-specific genes in the development of AN-like phenotype remains challenging and requires the combination of novel molecular tools and preclinical models. The activity-based anorexia (ABA) rat model recapitulates many aspects of the behavioural phenotypes of AN in humans and we have previously demonstrated that suppressing neural activity in the medial prefrontal cortex (mPFC)-nucleus accumbens shell (AcbSh) circuit prevented pathological weight loss in ABA rats. Here, we used a novel viral-based translating ribosome affinity purification (TRAP) technique to identify transcriptional changes within this neural pathway associated with susceptibility to ABA in female rats. We reveal 1424 differentially expressed genes between Susceptible and Resistant rats, highlighting important transcriptional changes associated with ABA within this pathway. The changes observed were independent of current calorie deficit and associated with metabolic, mitochondrial and neural functions. Further, we show that genes upregulated in Resistant rats were involved in mitochondrial function, while downregulated genes were associated with cytoskeletal, postsynaptic and axonal functions, supporting the hypothesis that hyperexcitability of cortico-striatal circuit function is a critical mediator of pathological weight loss in ABA. These findings provide novel insights into circuit-specific gene expression patterns that may contribute to susceptibility to developing AN in humans and highlight potential molecular targets for therapeutic intervention.

Introduction

Anorexia nervosa (AN) is a complex and serious illness characterised by a low body-mass index, behavioural disturbances such as inflexible thinking and compulsive behaviours, and higher mortality rates than most psychiatric disorders [1]. Available treatments have low rates of clinical success, in part, because renourishment protocols are not efficacious in addressing the deleterious drive to exacerbate dangerously low body weights [2]. Converging evidence from human neuroimaging studies and preclinical models suggest the involvement of altered neural circuit function, particularly aberrant activity within the prefrontal cortex (PFC) and striatum regions of the brain [3-6]. Interestingly, the largest genome-wide association study (GWAS) conducted to date (including ~17K cases and 55K controls) [7] suggests that genes associated with AN are enriched in similar brain regions, namely PFC and striatum [8], activity in which is associated with food reward valuation and cognitive flexibility [9, 10]. Although GWAS findings are informative, identifying strong hypotheses about their connections to specific genes, or how these specific genes are causal to changes in brain function or behaviour is not straightforward. Using a sophisticated complement of analytical tools including expression quantitative trait loci (eQTL) and chromosome conformation capture (Hi-C) interactions, 58 specific genes were identified to be significantly dysregulated in AN cases, with the clearest evidence for a role in the aetiology of AN for *Cadm1*, *Mgmt*, *Focp1* and *Ptbp2* [7], genes that are involved in cellular processes like receptor binding, DNA repair and cell-type specific gene transcription during development. However, it is important to recognise that by definition these findings are associations and may reflect variants and genes with no direct biological relevance to the causes of AN. Moreover, understanding the genetic predisposition of any neuropsychiatric disease is insufficient for informing novel prevention or treatment strategies if it does not pinpoint the brain regions or circuits where those genes have the greatest impact. Insight into the causal role of circuit-specific genes in the development and/or maintenance of AN-like phenotypes is now possible with novel molecular tools in combination with preclinical models.

Activity-based anorexia (ABA) is a biobehavioural rodent model that recapitulates many of the behavioural phenotypes of AN in humans, including voluntary food restriction and paradoxical hyperactivity in states of negative energy balance that leads to rapid reductions in body weight. Accordingly, the ABA model has been used for decades to gain mechanistic insight into the biological bases for AN, including predisposing factors [11-14]. The observation that when exposed to the same environmental conditions of ABA, both wild-type adolescent rats [15] and mice [16] consistently split into ‘Susceptible’ and ‘Resistant’ phenotypes makes this a particularly powerful model for understanding what differentiates individuals that go on to develop pathological weight loss and compulsive exercise from those that do not. Therefore, the ABA model could provide a valuable tool to dissect the causal involvement of genes associated with AN, but thus far its use has not shed sufficient light on the genetic determinants of AN [17]. We have previously shown that suppressing activity within a cortico-striatal neural circuit that extends between the medial prefrontal cortex

(mPFC) and nucleus accumbens shell (AcbSh) both prevents weight loss in ABA and improves cognitive flexibility in female rats [6]. This circuit is important in the context of AN-like behaviours because of its role in the suppression of learned stimulus-response behaviour (i.e. behaviour that is influenced by the consequences of actions) by regulating sensitivity to punishment [18]. Moreover, dysfunction in this circuit is reflected in the analogous human brain regions (PFC, ventral striatum) in individuals with AN, which may increase throughout the course of illness [19] and persist after weight recovery [3]. A caveat in interpreting our circuit-level findings arises from a subsequent study in which we examined flexible learning and susceptibility to ABA in the same (rat) subjects. Here, we showed that in fact *better* performance on the cognitive task predicted weight loss in ABA [20] suggesting a more nuanced role for cortico-striatal circuitry and reinforcement learning in the development of ABA and possibly the prodromal symptoms of AN in humans.

In order to interpret how disrupted neurochemistry and/or neural circuit function gives rise to the specific pathology of AN, the molecular phenotype that determines the functional output of the neural circuits involved needs to be identified. Traditional assessment of the genetic contributions to AN using targeted genetic knockout/down in animal models have yielded insufficient evidence to date for a molecular signature of AN [21], perhaps because of compensatory mechanisms that come into play when a gene construct is manipulated within an entire organism or brain region. It is also important in the context of a condition like AN, for which very little is known about the underlying genetic drivers, to perform an unbiased screen of gene expression within specific circuits of ABA rats, in order to reveal novel mechanisms. With this in mind, we utilised translating ribosome affinity purification (TRAP) technology, which allows the synthesis of molecular and neuroanatomical information by immunoprecipitation of translating mRNAs from any population of neurons that express enhanced green fluorescent protein (eGFP). In order identify differentially regulated genes *within a specific neural pathway* that modulates weight loss in ABA rats, we employed a dual viral approach, in which coincident injection of a retrogradely transporting Cre-expressing virus and a Cre-dependent TRAP construct (eGFP-tagged ribosome protein L10a; EGFPL10a) were injected into the AcbSh and mPFC, respectively. This allows eGFP-tagging of ribosomes, and in turn access to actively translating mRNA, specifically within neurons of the mPFC-AcbSh pathway. RNA sequencing of the immunoprecipitated polysomes was performed to identify a circuit-based genetic profile that is associated with Susceptibility or Resistance to ABA. This approach provides high resolution and specificity in the pursuit of understanding the *causes* of functional changes in reward and cognitive processes involved in pathological weight loss.

Materials and Methods

Animals and housing

All animals were obtained from the Monash Animal Research Platform (MARP; Clayton, VIC, Australia). Female Sprague-Dawley rats (*n*=28) were 7 weeks of age on arrival in the laboratory. Animals were group-housed and acclimated to the 12-hour light/dark cycle (lights off at 1100h) for 7 days in a temperature (22-24°C) and humidity (30-50%) controlled room before experiments commenced. A male rat was individually housed in all experimental rooms to facilitate synchronization of oestrous cycle of the female rats [22]. All experimental procedures (see **Figure 1** for timeline) were conducted in accordance with the Australian Code for the care and use of animals for scientific purposes and approved by the Monash Animal Resource Platform Ethics Committee (ERM 29143).

Stereotaxic surgeries

Stereotaxic surgeries were performed under anaesthesia (2.5-3% isoflurane in oxygen) using a stereotaxic apparatus (Kopf Instruments, CA, USA) and micropipettes pulled from borosilicate glass (0.64mm; Drummond Scientific, PA, USA) with a tip of ~40µm. All animals were injected bilaterally with 250nL of retro-Cre (AAVrg-pgk-Cre; Addgene, #24593) into AcbSh (from bregma and brain surface: anteroposterior: +1.6mm, mediolateral: ± 0.7mm, dorsoventral: -6.6mm), followed by bilateral injection of 250nL of the Cre-dependent TRAP construct (AAV5-FLEX-EGFPL10a; Addgene #98747) into the mPFC (from bregma and brain surface: anteroposterior: +2.8mm, mediolateral: ± 0.5mm, dorsoventral: -3.2mm). Viral constructs were infused over 5 minutes (50nl/min), with pipette tips left at the coordinates for a further 5 minutes to allow virus dispersal. Meloxicam (2mg/kg; Boehringer Ingelheim, Germany) was subcutaneously injected into animals during surgery. Suture clips were used to close the surgery sites. Animals were group-housed with *ad libitum* food and water access post-surgery for 7 days.

Activity-based anorexia (ABA)

Following recovery from surgery and sufficient time for viral expression (see **Supplementary Figure 1**), rats were individually housed in transparent living chambers with a removable food basket and a running wheel (Lafayette Instruments, IN, USA). Rats were allowed to habituate to the living chamber with *ad libitum* food access and locked running wheel for 1 day, followed by habituation to the unlocked running wheel for 7 days to determine baseline activity. Running wheel activity was recorded in revolutions by the Scurry Activity Wheel Software (Lafayette Instruments, IN, USA) with data extracted in 1h time bins. During ABA, food access was restricted to 90 minutes per days at the onset of dark phase (1100-1230h), with body weight measurements taken daily at 1100h. Running in the hour before the feeding window (1000-1100h) was considered as food anticipatory activity

104 (FAA) [6, 12]. Time restricted food access persisted for a maximum of 10 days or until animals
105 reached <80% of baseline body weight (ABA criterion), the baseline measure being that taken on
106 Day 0 (prior to the first food restriction period). Following body weight recovery to at least 100% of
107 baseline with *ad libitum* food access (minimum of 3 days to regain baseline weight), rats were
108 euthanised with 300mg/kg sodium pentobarbitone (Lethabarb; Virbac, Australia), followed by rapid
109 dissection of the mPFC region performed in dissection buffer containing 1x HBSS, 2.5mM HEPES-
110 KOH (pH=7.4), 35mM glucose, 4mM $NaHCO_3$ and 100 µg /ml cycloheximide (CHX). Dissected tissue
111 was snap frozen in liquid nitrogen and stored at -80 °C until use.

112 Translating Ribosome Affinity Purification (TRAP) assay

113 TRAP was performed based on previously described protocols [23, 24] [25]. To prepare the tissue
114 for extraction of EGFP-tagged polysomes, the tissue was homogenised with a hand pestle mixer in
115 lysis buffer [10 mM HEPES-KOH, 150 mM KCl, 5 mM MgCl2, 0.5 mM DTT, 100 µg/ml CHX, RNase
116 inhibitor (RNasin, Promega, 40u/µl) and protease inhibitors (Roche, 1 tablet/ml)], followed by
117 centrifugation at 2000g at 4°C for 10 minutes. The supernatant was then incubated with NP-40
118 working solution and DHPC on ice for 5 minutes, followed by centrifugation at 13,000 g for 10 minutes
119 at 4°C. Following centrifugation, polysomes were immunoprecipitated from the supernatant by
120 overnight incubation at 4°C with anti-GFP antibody-labelled Dynabeads (Invitrogen, California,
121 USA). The bound RNA was collected with a magnetic rack and washed with a KCl wash buffer (10
122 mM HEPES-KOH, 350 mM KCl, 5 mM MgCl2, 1% NP-40, 0.5 mM DTT, 100 µg/ml CHX), followed
123 by RNA extraction using the RNeasy Micro Kit (Qiagen, The Netherlands).

124 RNA Sequencing

125 Twelve samples were selected for sequencing according to weight loss profiles, in which equal
126 numbers (*n*=4/group) were either clearly Resistant to developing ABA, rapidly lost weight under
127 conditions of ABA and were removed from the experimental paradigm after 3-4 days (Susceptible)
128 or exhibited an Intermediate phenotype, in which they lost weight to reach the removal criterion but
129 more slowly than Susceptible rats (6-9 days). Total RNA samples underwent quality control by
130 bioanalyser and those selected for sequencing had quantitation and RNA integrity number (RIN)
131 scores between 3.0-9.6. The resulting library pool was QC'd by Qubit, Bioanalyzer and qPCR. It had
132 a mean size of 361bp at a concentration of 9.9nM. Sequencing was performed using NextSeq2000
133 on a P2 100cycle kit (cDNA reads generated 101nt), with read coverage up to 400M reads per run.
134 A novel RNA-Seq pipeline (Version 01/09/2021) was used on the final library pool, loaded at 1000pM
135 (based upon size adjusted qPCR) for on-board denaturation and clustering (Illumina Protocol;
136 1000000109376 v3 Nov2020) which resulted in a loading metric of 98.42 and 88.95% >Q30. 541.2
137 reads passed filter and 464 Million reads were assigned to indexes. Briefly, index is added during
138 initial pA priming and pooled samples amplified using template switching oligo. P5 is added by

139 tagmentation by Nextera transposase and PCR. On-board denaturing and clustering were
140 conducted using 1000pM of library pool. Parsing and base calling was conducted (Dragen
141 BCLConvert 3.7.4) and showed that Sample 22-2449 (Resistant) had the lowest amount of sample
142 with 6.5ng total RNA. Since all samples are pooled for the multiplex method, this amount was used
143 as starting amount for all samples. Libraries were made by individual first strand synthesis to add
144 the i7 index sequences indicated in **Supplementary Table 1**. Samples were pooled for subsequent
145 processing.

146 Analysis

147 The raw sequencing reads were adapter trimmed using Trim Galore (v0.6.7;
148 https://github.com/FelixKrueger/TrimGalore) with standard parameters. Reads were aligned to the
149 Rat reference genome (Rattus_norvegicus.mRatBN7) with STAR (v 2.7.9a) [26] and quantified using
150 Salmon (v 1.9.0) [27]. The reference genome was downloaded from Ensembl, along with the gene
151 annotation in a .gtf file. MultiQC (v 3.9.5) [28] was used to generate the summary of the final quality
152 metrics for all datasets. Differential expression analysis was carried out using edgeR [29] along with
153 the RUVseq [30] to remove unwanted noise in the data. Genes with 1 count per million in at least
154 three samples per group were selected to perform the tests of differential expression. Significant
155 differentially expressed genes (DEGs) were selected using log-fold-change of ±1 and FDR cut-off of
156 0.05 and were used for performing gene-set enrichment analysis (GSEA). The Rat Genome
157 Database pathway and gene ontology (GO) analysis utilities were used [31]. GSEA was used to
158 identify classes of genes that are over-represented in a large set of genes or proteins, and may have
159 an association with different phenotypes. GO analyses were summarized at the level of Biological
160 process (BP), Cellular Component (CC), and Molecular Function (MF). Pathway analysis results
161 were plotted using the online platform SRplot (http://www.bioinformatics.com.cn/SRplot) [32].
162 Specific details of quality metrics from the MultiQC report are available on request.

163 Statistical Analysis

164 Statistical analyses were performed using GraphPad Prism (GraphPad Software, San Diego, CA,
165 USA). Statistical significance was considered as $p<.05$. Analyses including two-tailed unpaired t-test,
166 one-way and two-way analysis of variance (ANOVA) with Tukey's or Bonferroni's post hoc multiple
167 comparisons were used according to the number of groups in the ABA data. Volcano plots displaying
168 DEGs and GO analyses for up and downregulated genes used a negative log FDR of >1.3 to
169 determine statistical significance ($p<.05$).

170 ## Results

171 Susceptible and Resistant rats demonstrate distinct behavioural phenotypes in ABA

172 In accordance with our previously characterized susceptibility criterion [5, 6, 15], Resistant rats
173 showed a slower body weight loss rate and maintained >80% of their baseline body weight for the
174 entire 10-day ABA exposure period [**Figure 2A-D; B**, p = 0.0045; **C**, Experimental day $F(10,74)$ =
175 15.0, $p < 0.0001$; ABA Susceptibility $F(1,10)$ = 12.5, p= 0.0054; **D**, p = 0.0037]. Consistent with their
176 ability to maintain body weight, Resistant rats consumed significantly more during the 90 minutes of
177 food access throughout the 10-day period [**Figure 2E-F**; **E**, Experimental day $F(9,63)$ = 9.46, p <
178 0.0001; ABA Susceptibility $F(1,10)$ = 2.59, p = 0.1384; **F**, p= 0.0099], but did not demonstrate an
179 increased level of food anticipatory activity (FAA; **Figure 2H**, p= .3029), contrary to previous reports
180 [6]. Resistant rats also maintained a relatively stable and moderate level of daily running wheel
181 activity, whereas Susceptible rats showed a clear activity spike at the onset of food restriction [**Figure**
182 **2G;** ABA: Experimental day $F(10,63)$ = 3.39, p = 0.0013; ABA Susceptibility $F(1,10)$ = 10.9, p=
183 0.007].

184 Differentially expressed genes align with data from GWAS and implicate both metabolic and synaptic
185 processes in pathological weight loss

186 Motivated by the complex roles of the cortico-striatal (mPFC-AcbSh) pathway during cognitive
187 flexibility *versus* reinforcement learning in ABA rats, next we investigated whether stable molecular
188 phenotypes in this pathway are associated with susceptibility to excessive exercise and weight loss.
189 To examine enduring (and perhaps intrinsic) transcriptomic differences within the mPFC-AcbSh
190 pathway between the two phenotypes, we harnessed the TRAP technology to selectively isolate
191 ribosome-bound mRNA from this pathway after body weight recovery (at least to 100% of baseline).
192 This approach was chosen to disambiguate compensatory mechanisms from possible circuit-specific
193 differences underlying susceptibility to ABA.

194 edgeR analysis between groups revealed 1424 differentially expressed genes (DEGs) between
195 Susceptible and Resistant rats, highlighting important transcriptional differences associated with
196 Resistance to ABA within this neural circuit ($-\log_{10}$FDR > 1.3, **Figure 3A**). To further understand the
197 biological significance of DEGs, gene ontology (GO) analysis revealed that DEGs were significantly
198 enriched in pathways related to oxidative phosphorylation and associated with neurodegenerative
199 diseases, including Parkinson's, Alzheimer's and Huntington's diseases (**Figure 3B)**. The major
200 molecular and cellular-related themes that emerged were in genes associated with mitochondrial
201 and cytoskeletal functions, cellular organisation and protein complex assembly (**Figure 3C-E)**. More
202 specifically, among these genes we found that upregulated genes were mainly involved in metabolic
203 processes (*Atp5mkl:* LogFC= 1.50*; Uqcr10*: LogFC= 1.32) and downregulated genes were involved
204 in cytoskeletal, postsynaptic and axonal functions (blue box; **Figure 3A**). Interestingly, 5 of the DEGs

205 were previously identified in GWAS as AN-associated genes [7]. Of these, *Zc3h10*, *Myl6*, *Ikzf4* and
206 *Erlec1* were upregulated in Resistant compared to Susceptible ABA rats, whereas *Smarcc2* was
207 downregulated in the Resistant group. These genes have functions in thermoregulation [33],
208 inflammatory responses [34] and endoplasmic reticulum stress [35].

209 A subgroup of Susceptible rats shows an "Intermediate" behavioural phenotype

210 Through our extensive experience with the ABA model, we have noticed phenotypic differences
211 within those rats Susceptible to ABA, particularly with respect to the *rate* of body weight loss. We
212 were therefore interested to understand whether differences in weight loss trajectory were related to
213 gene expression within this cortico-striatal pathway. Here, we distinguish Susceptible rats as those
214 that lost weight rapidly (i.e., reached the threshold for ABA susceptibility criterion in <4 days) and
215 Intermediate rats as those that still reached this criterion, albeit at a slower rate (**Figure 4A,-D; B**,
216 Intermediate vs Susceptible p = 0.0003; Intermediate vs Resistant p = 0.0096; Susceptible vs
217 Resistant p < 0.0001; **C**, p = 0.0079, **D**, Intermediate vs Susceptible p = 0.0002; Intermediate vs
218 Resistant p = 0.0049; Susceptible vs Resistant p < 0.0001). As described above, Resistant rats ate
219 significantly more when it was available than Susceptible rats [**Figure 4E-F**; **E,** Experimental day
220 $F(9,63)$ = 9.06, p < 0.0001; ABA Susceptibility $F(2,9)$ = 1.22, p = 0.3389; **F**, p = 0.0084], and
221 Intermediate rats consumed food in amounts between the two other groups. Interestingly, Resistant
222 and Intermediate rats engaged in the same level of food anticipatory activity, and although this was
223 reduced for Susceptible rats, the difference was not significant (**Figure 4H**, Intermediate vs
224 Susceptible p = 0.1550; Resistant vs Susceptible p =0.1430). Examination of the profiles of daily
225 running wheel activity showed a clear spike in activity at the onset of food restriction (dashed line)
226 for Susceptible rats, whereas Intermediate rats exhibit a more gradual increase in wheel running and
227 Resistant rats maintain a relatively constant rate of exercise [**Figure 4G** ABA: Experimental day
228 $F(10,63)$ = 3.58, p = 0.0008; ABA Susceptibility $F(2,9)$ = 8.24, p= 0.0092].

229 With this weight loss separation in mind, we examined the differences between two subgroups of
230 Susceptible rats compared to Resistant group and identified genes that were differentially expressed
231 between groups as well as those that overlapped. Overall, 651 DEGs were identified as overlapping
232 and substantially fewer DEGs were identified between Resistant and Intermediate subgroups than
233 those identified between Resistant and Susceptible, supporting their separation into discrete
234 categories (**Figure 5A**). Within these DEGs, 170 genes exclusively differed in the Intermediate
235 group, whereas 471 exclusively differed in the Susceptible group, further supporting the subgroup
236 delineation. Moreover, GO analysis revealed zero overlap between the two comparator groups in
237 terms of the top 15 biological processes, with Resistant and Susceptible rats mostly differing in genes
238 related to metabolic and mitochondrial functions, whereas Resistant and Intermediate rats were most
239 different by structural constituent and cytoskeletal functions. Specifically, the Intermediate group had
240 upregulated genes associated with neurodevelopmental disorders (e.g. *Shank1-3*) whereas the

241 Susceptible group were more genetically distinct to resistant rats, with upregulation of genes related
242 to synaptic function (e.g. *Camk2a*) and downregulation of genes involved in satiety (e.g. *Cck*),
243 inflammatory processes (e.g. *Ccl27*), and neuronal growth (e.g. *Bdnf*).

244 We were also interested in examining the up and downregulated DEGs between the Susceptible
245 and Intermediate subgroups compared to the Resistant group separately. Similar to the overlap in
246 DEGs, there was broad overlap between the Susceptible and Intermediate comparisons with
247 Resistant rats, in which 262 upregulated genes overlapped (**Figure 5B**) and 389 downregulated
248 genes overlapped (**Figure 5C**), with fewer DEGs identified between Resistant and Intermediate
249 subgroups than those identified between Resistant and Susceptible. In addition, 10 of the top 15
250 biological processes enriched for upregulated genes in both comparisons (Susceptible vs Resistant
251 and Intermediate vs Resistant) were the same, and 14 out of the top 15 biological processes enriched
252 for downregulated genes were common to both Susceptible and Intermediate comparisons with
253 Resistant rats.

254 <u>Susceptible and Intermediate subgroups may be differentiated by genes related to immune function</u>

255 To determine whether Susceptible and Intermediate rats showed DEG within this same pathway, we
256 directly compared the profile of these subgroups. Strikingly, no genes were differentially expressed
257 using the statistically corrected value for significance, indicating the two subgroups of "ABA
258 susceptible" rats do not display detectable differences in expression at the single gene level.
259 Nevertheless, we were interested to inspect up- and down-regulated genes before p-value
260 adjustments, given the known physiological and behavioural differences in these two subgroups.
261 Despite smaller fold changes, we see that Susceptible rats showed reduced expression the gene
262 encoding brain derived neurotrophic factor (*Bdnf*), in a similar manner when comparing Susceptible
263 and Resistant rats (**Figure 5A**), suggesting that low *Bdnf* expression may be a predictor of prominent
264 ABA susceptibility (**Figure 6A**). Furthermore, the gene encoding the dopamine-2 receptor subtype
265 (*Drd2*) was expressed in higher levels in those rats that lost weight more rapidly (**Figure 6A**), which
266 aligns with early work in which dopamine D2/3 receptor antagonism reduced the ABA phenotype
267 [36]. We also show a number of pathways that may be enriched in Susceptible rats that are related
268 to immune and inflammatory processes (**Figure 6B**), consistent with previous studies implicating
269 both immune system and cytokine signalling dysfunction in patients with AN [37, 38] and a
270 suggestion that circulating inflammatory markers are associated with discrete aspects of the ABA
271 phenotype [12].

272 Discussion

273 In this study, we used a novel viral-based TRAP technique to reveal transcriptional changes within
274 the cortico-striatal neuronal circuit that are associated with susceptibility to pathological weight loss
275 in ABA rats. These changes were associated with metabolic, mitochondrial and neuronal functions

276 and independent of current calorie deficit, since assessment occurred after weight recovery.
277 Upregulated genes in Resistant rats were enriched for mitochondrial function, in line with a recent
278 report of mitochondrial damage leading to oxidative stress in ABA rats [39], while downregulated
279 genes were involved in cytoskeletal, postsynaptic and axonal functions. Overall, these findings point
280 to *decreased excitability of the mPFC-AcbSh circuits* as a molecular signature that may confer
281 resistance to weight loss. This is consistent with our previous study showing that chemogenetic
282 *suppression* of this pathway caused resistance to pathological weight loss during ABA [6] and the
283 evidence of elevated activity of PFC regions in humans weight recovered from AN [3].

284 GWAS provide an excellent starting point for understanding the genetic architecture of complex
285 psychiatric disorders. Our study builds upon GWAS findings by investigating how gene expression
286 (i.e. the "message") is altered, rather than only the DNA (i.e. the "code"). One risk gene identified in
287 the largest GWAS investigation in AN cases [7], *Erlec1*, was significantly downregulated in
288 Susceptible compared to Resistant rats, but this was not significant when comparing Intermediate to
289 Resistant rats, suggesting that differences observed in weight loss trajectories might involve
290 dysregulated protein metabolism. Unfolded or misfolded proteins in the endoplasmic reticulum (ER)
291 are recognised by lectins including *Erlec1,* and an impairment in this recognition process could
292 disrupt ER homeostasis and cause tissue inflammation and endocrine dysregulation [40]. Notably,
293 *Erlec1* demonstrates reliable patterns of under-expression in central nodes within fear and reward
294 circuits, suggesting that genes linked with AN and vulnerability to rapid weight loss in ABA may
295 confer risk by altering processes related to fear- and reward-learning [41], consistent with reports of
296 persistent alterations in these processes after weight gain in AN [42] and with the role of this cortico-
297 striatal circuit in punishment learning (conditioned suppression) [18] .

298 In addition, genes associated with feeding behaviour and reward processing, including *Bdnf*, were
299 significantly downregulated in Susceptible rats compared to Resistant rats, but not for the
300 Intermediate weight losing subgroup. *Bdnf* mRNA expression is reduced in mPFC by scheduled
301 feeding in mice [43] and BDNF serum concentration is reduced in patients with AN [44]. These data
302 support the possibility that differences in weight loss trajectory in ABA could result from altered
303 reward-related feeding behaviour [5]. Intriguingly, the *Cck* gene, encoding the peptide hormone
304 cholecystokinin (CCK), was downregulated in both Susceptible and Intermediate rats, compared to
305 Resistant rats. The direction of effect here seems counterintuitive when considering the role of CCK
306 in signalling satiety [45], however it aligns with the observation of reduced circulating CCK in patients
307 with AN [46]. Thus, considering gene expression reported here is restricted to the cortico-stratal
308 circuitry, the downregulation we show may relate to the way that "higher order" cortical neurons that
309 express CCK mRNA in the rat [47] regulate appetite, through behavioural mechanisms such as
310 attention and impulse control.

311 The view that separate genetic profiles are involved in the genesis of rapid versus slower weight loss
312 in ABA rats is strengthened by the GSEA. Focusing on the top significantly enriched pathways

313 associated with the Susceptible or Intermediate ABA phenotype (see **Supplementary Figure 2**), it
314 is clear that dysregulation of genes associated with mitochondrial function (transport, dynamics and
315 homeostasis) is common to both "weight losing" groups, whereas dysregulation of genes involved in
316 neurodegenerative disease pathways was specific to rapid weight losers (i.e. Susceptible) and not
317 significantly associated with the Intermediate phenotype. Individuals that respond to ABA conditions
318 with rapid weight loss could be separated in future studies to investigate whether common
319 neurochemical disturbances seen in Parkinson's Disease (i.e. loss of dopamine neurons) or
320 Alzheimer's Disease (i.e. loss of acetylcholine neurons) play a role in the development or
321 maintenance of AN-like behaviours. A better understanding of these synergies could lead to more
322 effective treatments, in light of the fact that pharmacotherapies approved for neurodegenerative
323 diseases, such as donepezil (Aricept), have been proposed as a feasible possibility for treating AN
324 [48], and recent advances in understanding the AN-relevant mechanisms in mouse models [49].

325 Interestingly, although the Enriched Pathways and Biological Processes were distinct when
326 comparing Susceptible or Intermediate rats to Resistant rats, the Cellular Components and
327 Molecular Functions identified as significantly dysregulated were largely overlapping (see
328 **Supplementary Figures 3-4**). Surprisingly, no individual genes were significantly differentially
329 expressed by rats that lost weight rapidly compared to those with an Intermediate weight loss
330 phenotype, and the list of enriched GO terms between the two groups of "weight losers" was also
331 small, but included intracellular anatomical structure and protein binding functions (**Supplementary**
332 **Figure 5**). Thus, the differences in behavioural phenotype observed may be related to cell types or
333 circuits outside of the mPFC-AcbSh pathway (e.g. hypothalamus, brainstem) with indirect functional
334 consequences for this circuit. Indeed, our results suggest that differences between the two
335 subgroups could be caused by dysregulated inflammatory and immune functions. Inflammatory and
336 neurocognitive mechanisms may be intricately linked in the development of AN [50] and a risk locus
337 associated with AN is also associated with immune function [51]. Notably, the interleukin-6 (IL-6)
338 signalling and IL-6 family mediated signalling pathways were differentially regulated between
339 Intermediate rats and "rapid weight losers" (i.e. the Susceptible subgroup). This is particularly
340 interesting in light of our previous work that linked circulating IL-6 levels prior to ABA exposure with
341 the extent of weight loss, but only in rats resistant to developing ABA [12]. This finding should be
342 considered in the context that central and circulating levels of proinflammatory cytokines do not
343 always align and there are changes in IL-6 that occur as a result of excessive exercise and calorie
344 restriction independently and in a tissue-specific manner [52, 53]. Specifically, with respect to AN,
345 IL-6 levels might also be affected by illness duration and current body weight. While elevated serum
346 level of IL-6 is reported in patients with AN and it tends to normalise with treatment [37], the level of
347 IL-6 remains lower than healthy controls after weight restoration in a younger population of patients
348 [54].

349 Consistent with the significant co-morbidity between AN and psychiatric disorders including
350 depression, anxiety, substance use and obsessive-compulsive disorder (OCD) [55], genetic
351 correlations between these have also been revealed via single-nucleotide polymorphism (SNP)-
352 based methods. In particular, AN has the strongest (positive) genetic correlation with OCD [7] and
353 shares similar alterations in PFC expression [8], suggesting a common dysregulated functional
354 pathway. Direct evidence of genome-wide significant risk that is shared between AN and OCD has
355 not been identified, however, several genes have been suggested to drive the association, including
356 *Lrrc16a* and *Kit* [56], both involved in cell signalling pathways within the gastrointestinal tract.
357 Moreover, 109 pleiotropic loci were identified in a cross-disorder GWAS of psychiatric disorders
358 (including AN and OCD), in which the *Dcc* gene, the product of which plays a key role in guiding
359 axonal growth during development, was significantly associated with all eight psychiatric disorders
360 [57]. In addition, this study identified common genetic associations between AN and major
361 psychiatric disorders including schizophrenia, bipolar disorder and major depression, as well as
362 psychological traits including mood instability, neuroticism and intelligence, of which several
363 (*Csnk2b, Ctsa, Gpx1, P4htm and Tcf7l2)* were differentially expressed by the Susceptible and
364 Resistant rats, suggesting that the ABA model might capture genetic underpinnings of other
365 psychiatric traits that predispose individuals to AN. Despite the fact that the most translatable feature
366 of the ABA model is the development of compulsive exercise, which is an intermediate phenotype of
367 shared genetic risk for both OCD and AN [58], the putative genes that link AN to OCD were not found
368 to be differentially dysregulated in the present study. This could be due to the fact that specific risk
369 loci shared by AN and OCD have yet to be pinpointed [59] or that excessive exercise is driven not
370 by altered mPFC-AcbSh pathway activity but by disrupted function in other cortico-striatal pathways,
371 for example, those terminating in the dorsal striatum [60].

372 Although this study reveals genetic changes between Susceptible and Resistant rats that are
373 independent from current body weight state, we note that a major limitation is the inability to
374 differentiate causes and consequences of weight loss. Despite this, our results support the use of
375 the ABA model in investigating causal genetic factors to AN and provide directions for the
376 development of translationally relevant genetic models of AN. It is important to recognise that AN,
377 like most neuropsychiatric disorders, is by no means a monogenic disorder, and an understanding
378 of causal genetics derived from animal models will require assessment of a complex complement of
379 genetic drivers, acting in specific brain regions, that cannot be understood through global knockout
380 or knockin approaches. Thus, developing novel genetic models that incorporate ABA with specific
381 and inducible manipulations of AN-associated genes, or genetic variants such as copy number
382 variants (CNVs; [61]) or short structural variants (SSVs; [62]) could provide a better opportunity for
383 understanding the causal relationship between genetic factors, altered cognitive functions and
384 feeding or exercise pathologies.

385 In conclusion, this study suggests that weight loss in ABA results from hyperexcitability in this cortico-
386 striatal pathway, which is normalised in rats resistant to weight loss. The increased expression of
387 axonal and synaptic genes could indicate that too much neuronal activity in this circuit may cause
388 maladaptive behaviour. Future studies should aim to validate this interpretation with circuit-based
389 studies that include markers of pre- and post-synaptic densities, in which the hypothesis would be
390 that a greater "synaptic load" would be colocalised with the mPFC-AcbSh projecting cells in ABA
391 Susceptible compared to Resistant rats. In addition, it could be worthwhile to expose animals
392 expressing the circuit-TRAP construct used here to multiple "rounds" of ABA conditions, in order to
393 better understand the molecular drivers of weight loss stability and relapse.

394 Acknowledgements

395 We acknowledge the technical assistance with quality control and novel RNA sequencing pipelines
396 developed and performed by Dr Trevor Wilson, Monash Health Translational Precinct, Medical
397 Genomics Facility. We acknowledge the Monash Microimaging Platform for infrastructure used to
398 obtain immunofluorescence micrographs. We also acknowledge Biorender.com for elements of the
399 figure schematics.

References

1. Chesney, E., G.M. Goodwin, and S. Fazel, *Risks of all-cause and suicide mortality in mental disorders: a meta-review.* World Psychiatry, 2014. **13**(2): p. 153-60.
2. Watson, H.J. and C.M. Bulik, *Update on the treatment of anorexia nervosa: review of clinical trials, practice guidelines and emerging interventions.* Psychol Med, 2013. **43**(12): p. 2477-500.
3. Ehrlich, S., et al., *Elevated cognitive control over reward processing in recovered female patients with anorexia nervosa.* J Psychiatry Neurosci, 2015. **40**(5): p. 307-15.
4. Cha, J., et al., *Abnormal reward circuitry in anorexia nervosa: A longitudinal, multimodal MRI study.* Human Brain Mapping, 2016. **37**(11): p. 3835-3846.
5. Foldi, C.J., L.K. Milton, and B.J. Oldfield, *The Role of Mesolimbic Reward Neurocircuitry in Prevention and Rescue of the Activity-Based Anorexia (ABA) Phenotype in Rats.* Neuropsychopharmacology, 2017. **42**(12): p. 2292-2300.
6. Milton, L.K., et al., *Suppression of Corticostriatal Circuit Activity Improves Cognitive Flexibility and Prevents Body Weight Loss in Activity-Based Anorexia in Rats.* Biol Psychiatry, 2021. **90**(12): p. 819-828.
7. Watson, H.J., et al., *Genome-wide association study identifies eight risk loci and implicates metabo-psychiatric origins for anorexia nervosa.* Nat Genet, 2019. **51**(8): p. 1207-1214.
8. Song, W., et al., *Dissection of the Genetic Association between Anorexia Nervosa and Obsessive-Compulsive Disorder at the Network and Cellular Levels.* Genes (Basel), 2021. **12**(4).
9. Cox, J. and I.B. Witten, *Striatal circuits for reward learning and decision-making.* Nature Reviews Neuroscience, 2019. **20**(8): p. 482-494.
10. Joshi, A., et al., *Role of the striatal dopamine, GABA and opioid systems in mediating feeding and fat intake.* Neuroscience & Biobehavioral Reviews, 2022. **139**: p. 104726.
11. Barbarich-Marsteller, N.C., et al., *Identifying novel phenotypes of vulnerability and resistance to activity-based anorexia in adolescent female rats.* Int J Eat Disord, 2013. **46**(7): p. 737-46.
12. Milton, L.K., et al., *In pursuit of biomarkers for predicting susceptibility to activity-based anorexia in adolescent female rats.* Int J Eat Disord, 2022. **55**(5): p. 664-677.
13. Carrera, O., E. Gutiérrez, and R.A. Boakes, *Early handling reduces vulnerability of rats to activity-based anorexia.* Dev Psychobiol, 2006. **48**(7): p. 520-7.
14. Hancock, S. and V. Grant, *Early maternal separation increases symptoms of activity-based anorexia in male and female rats.* J Exp Psychol Anim Behav Process, 2009. **35**(3): p. 394-406.
15. Milton, L.K., B.J. Oldfield, and C.J. Foldi, *Evaluating anhedonia in the activity-based anorexia (ABA) rat model.* Physiol Behav, 2018. **194**: p. 324-332.
16. Beeler, J.A. and N.S. Burghardt, *Activity-based Anorexia for Modeling Vulnerability and Resilience in Mice.* Bio Protoc, 2021. **11**(9): p. e4009.
17. Foldi, C.J., *Taking better advantage of the activity-based anorexia model.* Trends in Molecular Medicine, 2024. **30**(4): p. 330-338.
18. Piantadosi, P.T., D.C.M. Yeates, and S.B. Floresco, *Prefrontal cortical and nucleus accumbens contributions to discriminative conditioned suppression of reward-seeking.* Learn Mem, 2020. **27**(10): p. 429-440.
19. Fladung, A.K., et al., *Role of the ventral striatum in developing anorexia nervosa.* Transl Psychiatry, 2013. **3**(10): p. e315.
20. Huang, K., et al., *Rapid, automated, and experimenter-free touchscreen testing reveals reciprocal interactions between cognitive flexibility and activity-based anorexia in female rats.* Elife, 2023. **12**.
21. Scharner, S. and A. Stengel, *Animal Models for Anorexia Nervosa—A Systematic Review.* Frontiers in Human Neuroscience, 2021. **14**.
22. Cora, M.C., L. Kooistra, and G. Travlos, *Vaginal Cytology of the Laboratory Rat and Mouse: Review and Criteria for the Staging of the Estrous Cycle Using Stained Vaginal Smears.* Toxicol Pathol, 2015. **43**(6): p. 776-93.

23. Heiman, M., et al., *Cell type–specific mRNA purification by translating ribosome affinity purification (TRAP).* Nature Protocols, 2014. **9**(6): p. 1282-1291.
24. Ip, C.K., et al., *Amygdala NPY Circuits Promote the Development of Accelerated Obesity under Chronic Stress Conditions.* Cell Metabolism, 2019. **30**(1): p. 111-128.e6.
25. Nectow, A.R., et al., *Rapid Molecular Profiling of Defined Cell Types Using Viral TRAP.* Cell Rep, 2017. **19**(3): p. 655-667.
26. Dobin, A., et al., *STAR: ultrafast universal RNA-seq aligner.* Bioinformatics, 2013. **29**(1): p. 15-21.
27. Patro, R., et al., *Salmon provides fast and bias-aware quantification of transcript expression.* Nat Methods, 2017. **14**(4): p. 417-419.
28. Ewels, P., et al., *MultiQC: summarize analysis results for multiple tools and samples in a single report.* Bioinformatics, 2016. **32**(19): p. 3047-8.
29. Robinson, M.D., D.J. McCarthy, and G.K. Smyth, *edgeR: a Bioconductor package for differential expression analysis of digital gene expression data.* Bioinformatics, 2010. **26**(1): p. 139-40.
30. Risso, D., et al., *Normalization of RNA-seq data using factor analysis of control genes or samples.* Nat Biotechnol, 2014. **32**(9): p. 896-902.
31. Petri, V., et al., *The Rat Genome Database Pathway Portal.* Database, 2011. **2011**: p. bar010.
32. Tang, D., et al., *SRplot: A free online platform for data visualization and graphing.* PLoS One, 2023. **18**(11): p. e0294236.
33. Yi, D., et al., *Zc3h10 Acts as a Transcription Factor and Is Phosphorylated to Activate the Thermogenic Program.* Cell Rep, 2019. **29**(9): p. 2621-2633.e4.
34. Liu, W., et al., *RNF138 inhibits late inflammatory gene transcription through degradation of SMARCC1 of the SWI/SNF complex.* Cell Reports, 2023. **42**(2).
35. Misiewicz, M., et al., *Identification of a Novel Endoplasmic Reticulum Stress Response Element Regulated by XBP1 *.* Journal of Biological Chemistry, 2013. **288**(28): p. 20378-20391.
36. Klenotich, S.J., et al., *Dopamine D2/3 receptor antagonism reduces activity-based anorexia.* Transl Psychiatry, 2015. **5**(8): p. e613.
37. Dalton, B., et al., *A meta-analysis of cytokine concentrations in eating disorders.* J Psychiatr Res, 2018. **103**: p. 252-264.
38. Pisetsky, D.S., et al., *The expression of cytokines and chemokines in the blood of patients with severe weight loss from anorexia nervosa: an exploratory study.* Cytokine, 2014. **69**(1): p. 110-5.
39. Bhasin, H., et al., *Activity-based anorexia in adolescent female rats causes changes in brain mitochondrial dynamics.* Physiology & Behavior, 2023. **261**: p. 114072.
40. Lemmer, I.L., et al., *A guide to understanding endoplasmic reticulum stress in metabolic disorders.* Molecular Metabolism, 2021. **47**: p. 101169.
41. Murray, S.B., et al., *Brain-based gene expression of putative risk genes for anorexia nervosa.* Mol Psychiatry, 2023. **28**(6): p. 2612-2619.
42. Murray, S.B., et al., *Fear as a translational mechanism in the psychopathology of anorexia nervosa.* Neuroscience & Biobehavioral Reviews, 2018. **95**: p. 383-395.
43. Ho, E.V., et al., *Activity-Based Anorexia Alters the Expression of BDNF Transcripts in the Mesocorticolimbic Reward Circuit.* PLoS One, 2016. **11**(11): p. e0166756.
44. Nilsson, I.A.K., et al., *Aberrant inflammatory profile in acute but not recovered anorexia nervosa.* Brain, Behavior, and Immunity, 2020. **88**: p. 718-724.
45. Moran, T.H., *Cholecystokinin and satiety: current perspectives.* Nutrition, 2000. **16**(10): p. 858-865.
46. Baranowska, B., et al., *Disturbed release of gastrointestinal peptides in anorexia nervosa and in obesity.* Diabetes, Obesity and Metabolism, 2000. **2**(2): p. 99-103.
47. Burgunder, J.M. and W.S. Young, 3rd, *Cortical neurons expressing the cholecystokinin gene in the rat: distribution in the adult brain, ontogeny, and some of their projections.* J Comp Neurol, 1990. **300**(1): p. 26-46.
48. Bucay, A.H., *Donepezil (aricept) as a treatment for anorexia nervosa: a very feasible therapeutic possibility.* Expert Opinion on Investigational Drugs, 2009. **18**(5): p. 569-571.

49. Favier, M., et al., *Cholinergic dysfunction in the dorsal striatum promotes habit formation and maladaptive eating.* (1558-8238 (Electronic)).
50. Brooks, S.J., et al., *A neuroinflammatory compulsivity model of anorexia nervosa (NICAN).* Neuroscience & Biobehavioral Reviews, 2024. **159**: p. 105580.
51. Duncan, L., et al., *Significant Locus and Metabolic Genetic Correlations Revealed in Genome-Wide Association Study of Anorexia Nervosa.* Am J Psychiatry, 2017. **174**(9): p. 850-858.
52. da Rocha, A.L., et al., *The proinflammatory effects of chronic excessive exercise.* Cytokine, 2019. **119**: p. 57-61.
53. Okita, N., et al., *Differential responses of white adipose tissue and brown adipose tissue to caloric restriction in rats.* Mechanisms of Ageing and Development, 2012. **133**(5): p. 255-266.
54. Specht, H.E., et al., *Lower serum levels of IL-1β and IL-6 cytokines in adolescents with anorexia nervosa and their association with gut microbiota in a longitudinal study.* Front Psychiatry, 2022. **13**: p. 920665.
55. Salbach-Andrae, H., et al., *Psychiatric comorbidities among female adolescents with anorexia nervosa.* Child Psychiatry Hum Dev, 2008. **39**(3): p. 261-72.
56. Yilmaz, Z., et al., *Examination of the shared genetic basis of anorexia nervosa and obsessive-compulsive disorder.* Mol Psychiatry, 2020. **25**(9): p. 2036-2046.
57. Lee, P.H., et al., *Genomic Relationships, Novel Loci, and Pleiotropic Mechanisms across Eight Psychiatric Disorders.* Cell, 2019. **179**(7): p. 1469-1482.e11.
58. Yilmaz, Z., et al., *Predicting eating disorder and anxiety symptoms using disorder-specific and transdiagnostic polygenic scores for anorexia nervosa and obsessive-compulsive disorder.* Psychol Med, 2023. **53**(7): p. 3021-3035.
59. Bulik, C.M., et al., *Genetics and neurobiology of eating disorders.* Nat Neurosci, 2022. **25**(5): p. 543-554.
60. Conn, K., et al., *A transdiagnostic and translational framework for delineating the neuronal mechanisms of compulsive exercise in anorexia nervosa.* International Journal of Eating Disorders, 2024. **57**(7): p. 1406-1417.
61. Walker, A., et al., *Genome-wide copy number variation association study in anorexia nervosa.* Molecular Psychiatry, 2024.
62. Berthold, N., et al., *Bridging the gap: Short structural variants in the genetics of anorexia nervosa.* Int J Eat Disord, 2022. **55**(6): p. 747-753.

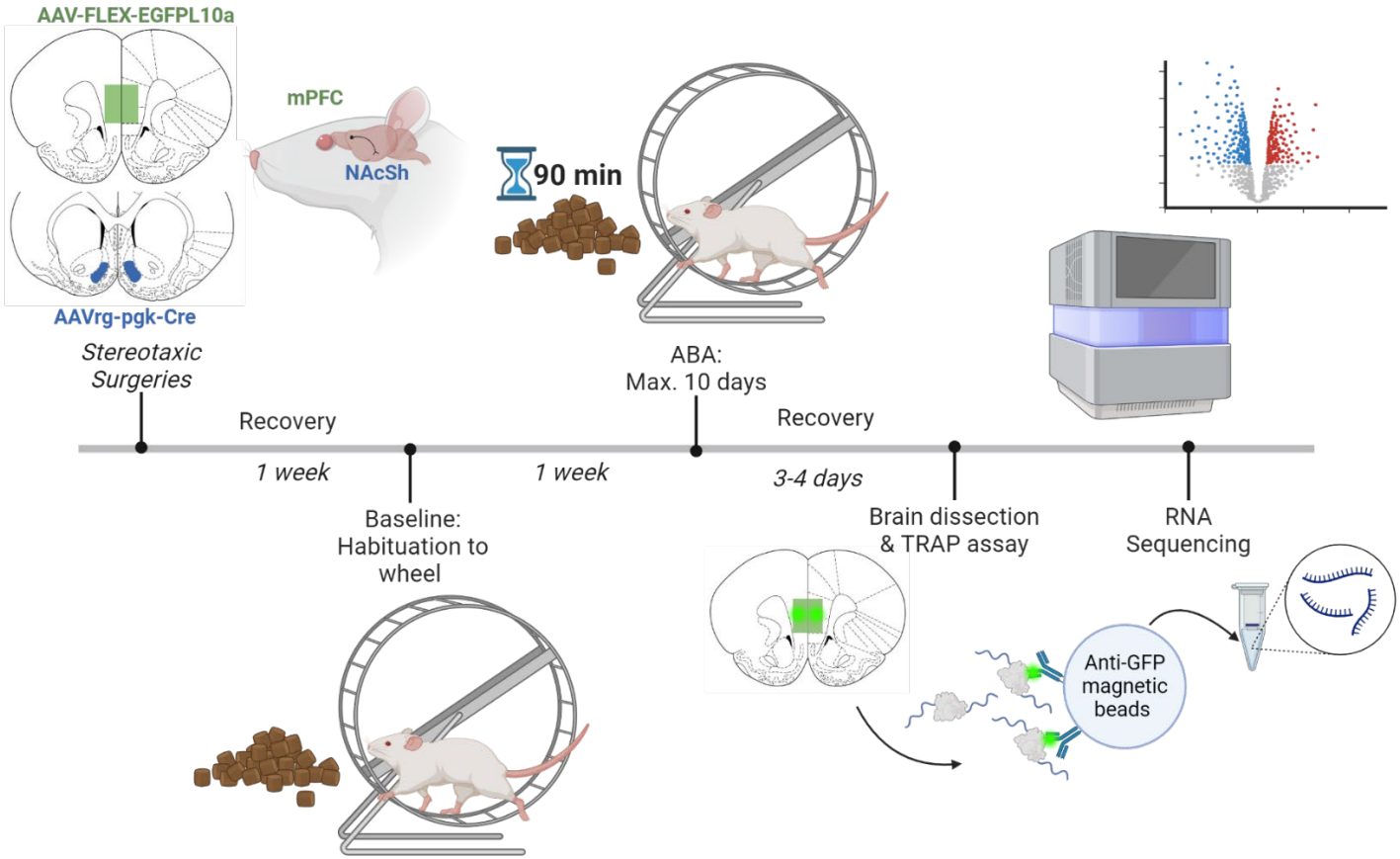

Figure 1. Timeline of experiments. Female Sprague-Dawley rats were injected with AAV-FLEX-EGFPL10a into medial prefrontal cortex (mPFC) and retrogradely transporting AAVrg-pgk-Cre into nucleus accumbens shell (NAcSh). Following one week of recovery, rats were habituated to running wheels with *ad libitum* food access for 7 days to determine baseline body weight and running wheel activity. Activity-based anorexia (ABA) conditions commenced with food access limited to 90 minutes per day and lasted for a maximum of 10 days or until rats reached <80% baseline body weight. Rats were allowed to recover to baseline body weight with *ad libitum* food access for 3 to 4 days before brain dissection. Tissue from mPFC was used in the TRAP assay to extract labelled RNA, followed by RNA sequencing and analyses.

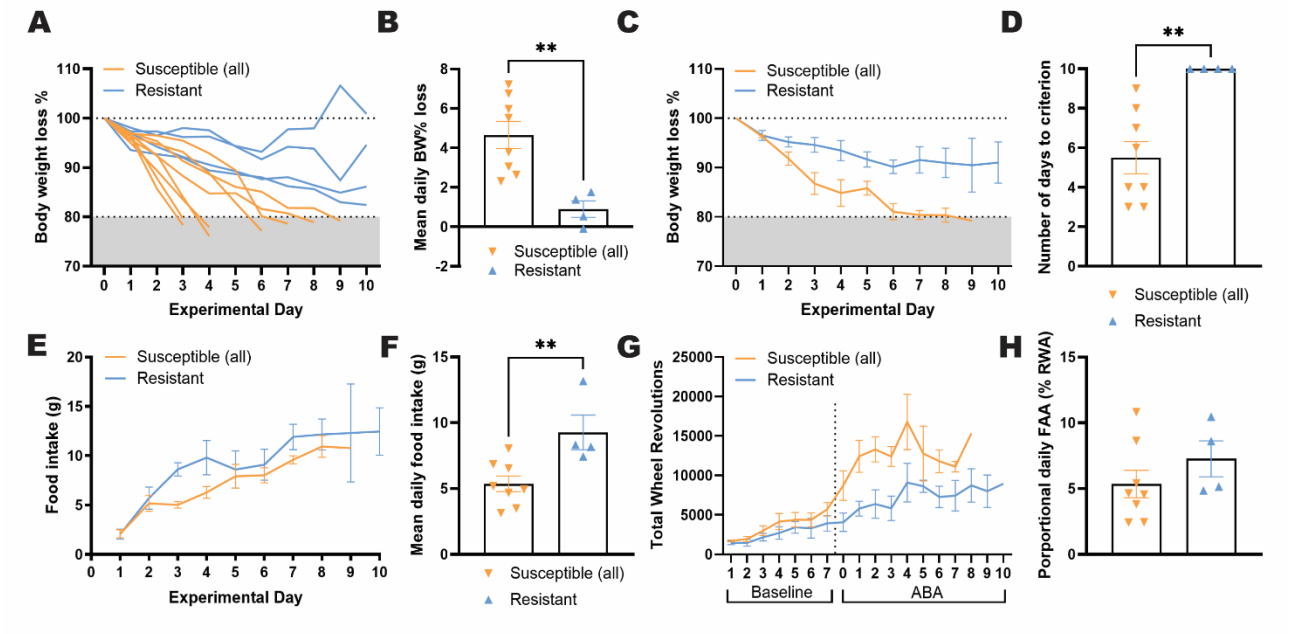

Figure 2. Primary ABA outcome measures for rats Susceptible and Resistant to weight loss. As expected based on susceptibility criteria, Resistant rats were able to maintain body weight above the threshold of 80% baseline body weight for the entire 10-day period, whereas Susceptible rats were not (**A)** and demonstrated a more rapid weight loss rate [**B-D**; **B**, $t(10) = 3.640$, $p = 0.0045$; **C**, Experimental day $F(10,74) = 15.0$, $p < 0.0001$; ABA Susceptibility $F(1,10) = 12.5$, $p = 0.0054$; **D**, $t(10) = 3.770$, $p = 0.0037$]. Resistant rats also ate more food within the time window than Susceptible rats during the 10-day ABA period [**E-F; E,** Experimental day $F(9,63) = 9.46$, $p < 0.0001$; ABA Susceptibility $F(1,10) = 2.59$, $p = 0.1384$; **F**, $t(10) = 3.173$, $p = 0.0099$]. Overall running wheel activity was significantly higher in Susceptible rats [**G;** Baseline: Experimental day $F(6,60) = 9.01$, $p < 0.0001$; ABA Susceptibility $F(1,10) = 1.05$, $p = 0.3288$; Interaction $F(6,60) = 0.420$, $p = 0.8629$; ABA: Experimental day $F(10,63) = 3.39$, $p = 0.0013$; ABA Susceptibility $F(1,10) = 10.9$, $p = 0.0079$], contributing to their improved body weight maintenance. However, motivated running in anticipation of food [**H**, $t(10) = 1.086$, $p = 0.3029$] was not significantly elevated in Resistant rats. Grouped data show mean ± SEM, with individual data point on the bar graphs. ** $p < 0.01$. ABA, Activity-based anorexia; BW, Body weight; FAA, Food anticipatory activity.

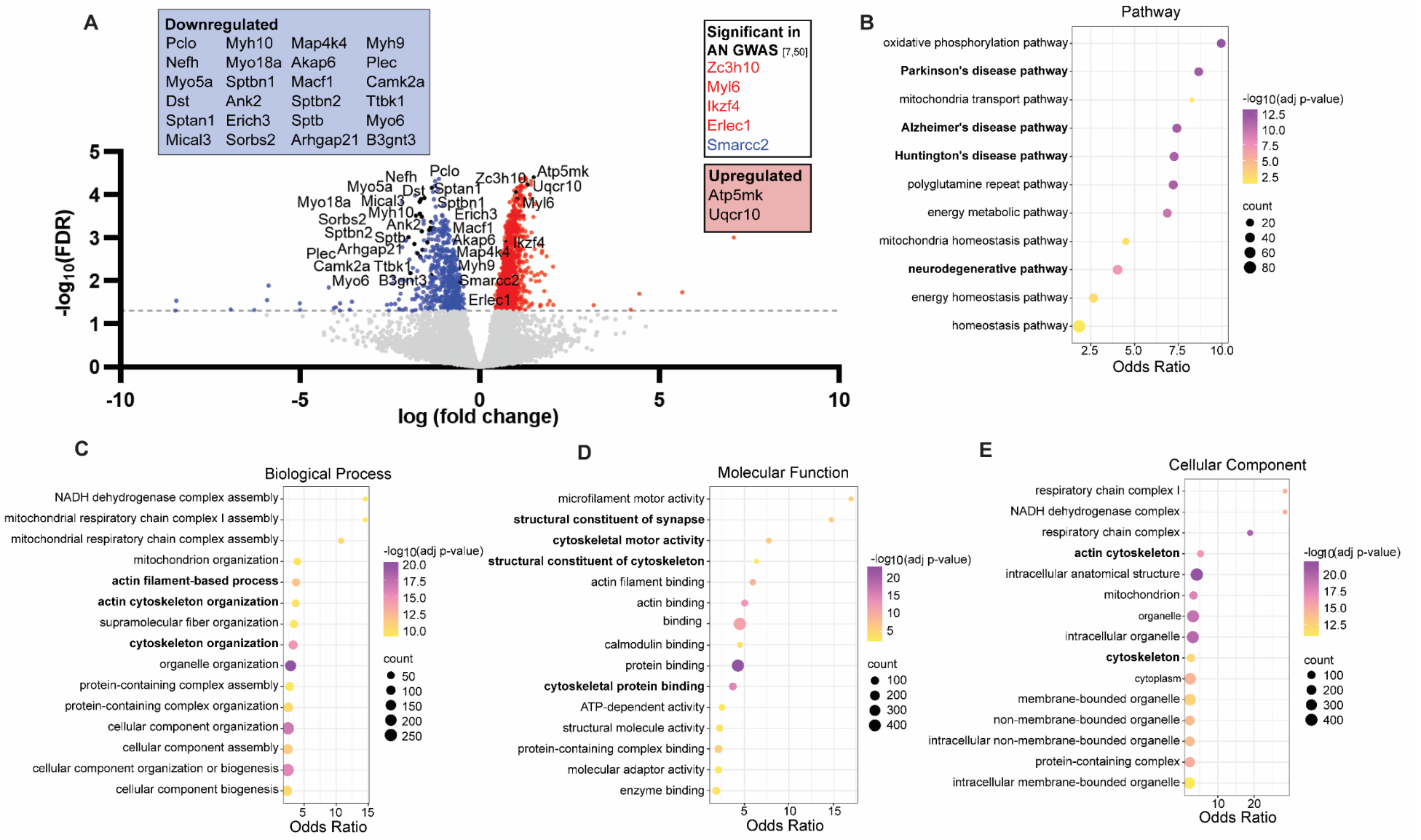

Figure 3: Rats that are Resistant to ABA show distinct gene expression profiles in striatum projecting mPFC neurons compared to Susceptible rats. Volcano plot of 1424 significant differentially expressed genes (DEGs) between Susceptible and Resistant rats (**A**). Grey dashed

line represents a $-\log_{10}$(FDR) = 1.3, the threshold for statistical significance (p <.05). The blue dots denote all significantly downregulated genes observed in the Resistant, the red dots denote all significantly upregulated genes in the Resistant group, and grey dots represent genes that differed in expression between groups that did not reach statistical significance. Gene names are indicated for the most significant and stable (i.e. the least between-sample variability) upregulated (2) or downregulated (24) genes and the 5 genes that are significant in human genome-wide associated studies for anorexia nervosa (Watson et al., 2019 & Duncan et al., 2017). Pathways that were significantly (corrected p-value < 0.05) enriched in Susceptible vs. Resistant rats are involved in metabolic functions and neurodegenerative diseases (**B**). The top 15 biological process (**C**), molecular function (**D**), and cellular component (**E**) Gene Ontology (GO) terms enriched in DEGs predominantly relate to mitochondrial and cytoskeletal functions. The vertical axis of the bubble plots represents the pathway name or GO term, which is used to describe function of a gene. The horizontal axis represents the Odds Ratio, which is the likelihood of a pathway or GO term to be associated with a set of genes of interest compared to a reference set of genes. A higher odds ratio represents a stronger enrichment of the term or pathway. The colour scale for each bubble plot (**B-E**) indicates different thresholds of the p-value, whereby a lighter colour represents a greater significance. In addition, the bubbles size represents the number of genes observed to be differentially expressed within each pathway or term. Terms with a corrected p-value < 0.05 and an odds ratio between 1.3 and 40 were included.

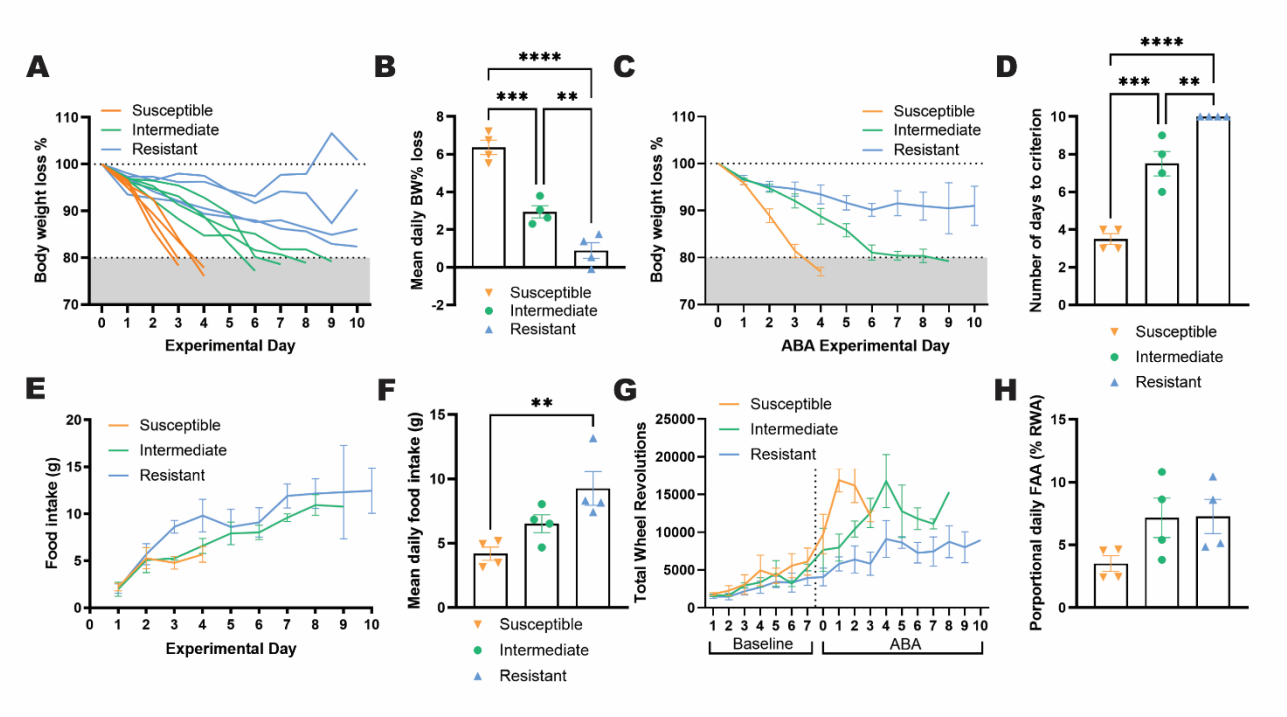

Figure 4: Separation of ABA rats based on trajectory of weight loss reveals an intermediate phenotype. While Susceptible rats lost weight rapidly, Intermediate rats reached the threshold for ABA susceptibility criterion, albeit at a slower rate [**A-D** , **B**, $F(2,9) = 54.3$, $p < 0.0001$, Intermediate vs Susceptible $p = 0.0003$; Intermediate vs Resistant $p = 0.0096$; Susceptible vs Resistant $p < 0.0001$; **C**, Experimental day $F(10,74) = 15.3$, $p < 0.0001$, ABA Susceptibility $F(2,9) = 8.68$, $p = 0.0079$; **D**, $F(2,9) = 64.5$, $p < 0.0001$, Intermediate vs Susceptible $p = 0.0002$; Intermediate vs Resistant $p = 0.0049$; Susceptible vs Resistant $p < 0.0001$] and engaged in feeding at levels between the two other groups [but not significantly different to either; **E-F**;**E,** Experimental day $F(9,63) = 9.06$, $p < 0.0001$; ABA Susceptibility $F(2,9) = 1.22$, $p = 0.3389$;**F** $F(2,9) = 7.84$, $p = 0.0107$, Resistant > Intermediate $p = 0.1364$, Intermediate > Susceptible $p = 0.219$]. Examination of the profiles of daily running wheel activity showed a clear spike in activity at the onset of food restriction (dashed line) for Susceptible rats, whereas Intermediate rats exhibit a more gradual increase in wheel running [**G,** Baseline: Experimental day $F(6, 54) = 11.50$, $p < 0.0001$; ABA Susceptibility $F(2, 9) = 0.7325$ $p= 0.5073$; Interaction $F(12,54) = 0.7031$, $p = 0.7415$; ABA: Experimental day $F(10,63) = 3.58$, $p = 0.0008$; ABA Susceptibility $F(2,9) = 8.24$, $p= 0.0092$]. Interestingly, Resistant and Intermediate rats engaged in the same level of motivated running in anticipation of food (FAA) [**H**, $F(2,9) = 2.889$, $p = 0.1074$, Intermediate vs Susceptible $p = 0.1550$, Resistant vs Intermediate $p = 0.9984$]. Grouped data show mean ± SEM, with individual data point on the bar graphs. ** $p < 0.01$, *** $p < 0.001$, ****$p < 0.0001$. ABA, Activity-based anorexia; BW, Body weight; FAA, Food anticipatory activity.

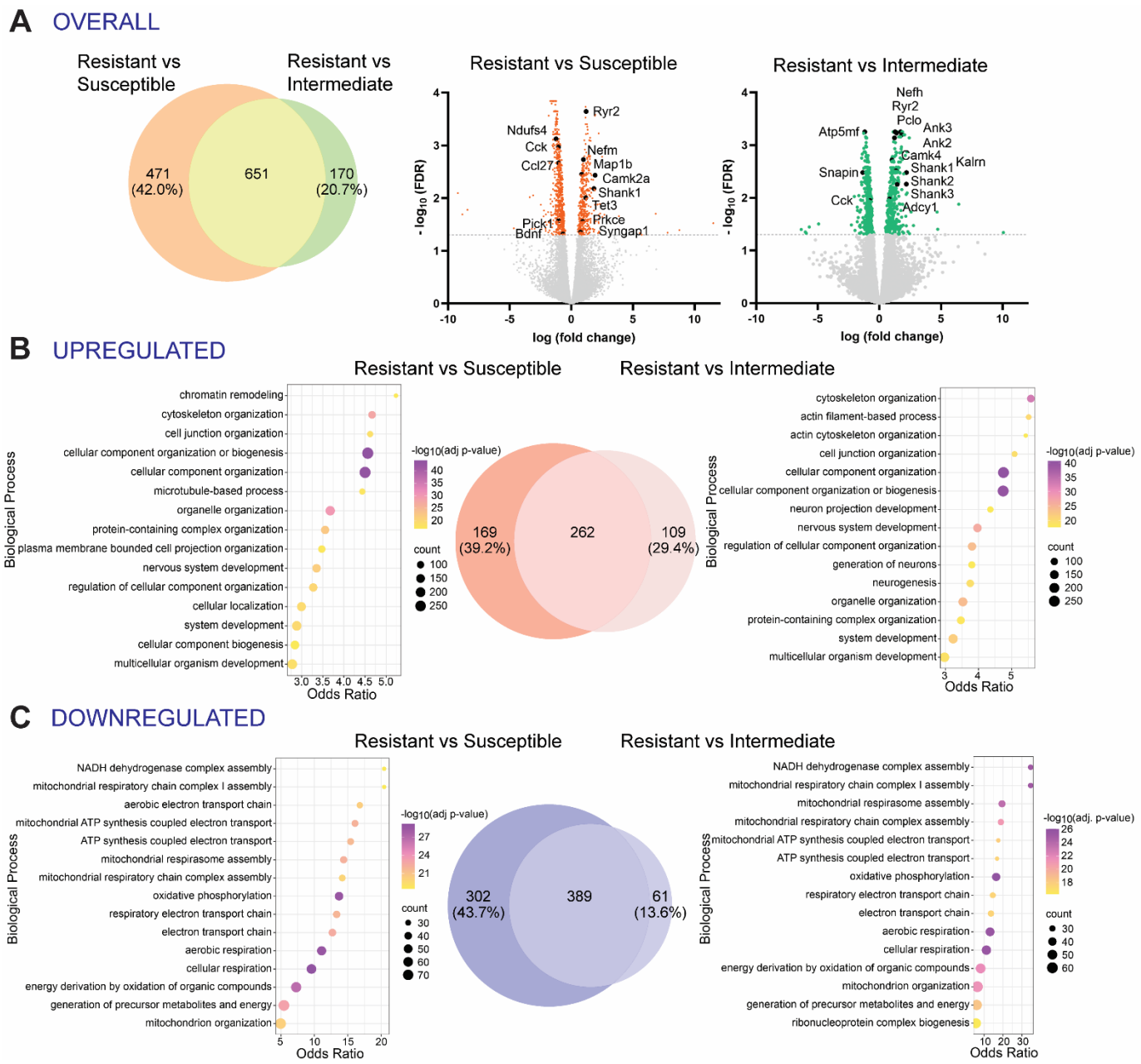

Figure 5: Gene expression profiles for ABA Resistant rats, compared to Susceptible or Intermediate subgroups. Venn diagram shows overlap of differentially expressed genes (DEGs) in Susceptible and/or Intermediate compared to Resistant rats (**A**), noting a large group of genes (651) are common to both comparisons and that there are fewer DEGs exclusively found in the Resistant vs. Intermediate comparison (170) than the Resistant vs Susceptible comparison (471). Volcano plots of DEGs for Resistant compared to Susceptible or Intermediate subgroup. The significant DEGs [$-\log_{10}$(FDR) > 1.3] are indicated in orange or green, with gene names of interest indicated for genes that are related to neurodevelopmental disorders, synaptic function, satiety, inflammatory processes and feeding behaviours, all processes relevant to the development of ABA in rats and AN in humans. Venn diagram shows overlapping of DEGs that are upregulated in Susceptible (left) or Intermediate (right) rats compared to Resistant rats (**B**), with 39.2% of upregulated DEGs that are exclusive to Susceptible but not Intermediate. 10 of the Top 15 biological process terms enriched in

the upregulated DEGs common between the two comparisons (i.e. Susceptible vs Resistant and Intermediate vs Resistant - see bubble plots). With respect to downregulated DEGs, the Venn diagram shows that 43.7% of identified genes are exclusive to the Susceptible vs Resistant group comparison and do not overlap with those in the Intermediate vs Resistant group comparison (**C**). Here, 14 of the Top 15 biological process terms enriched in the downregulated DEGs are common to both groups (see bubble plots), which are involved in metabolic and mitochondrial functions and suggests that these processes are a shared feature of both “weight losing” groups.

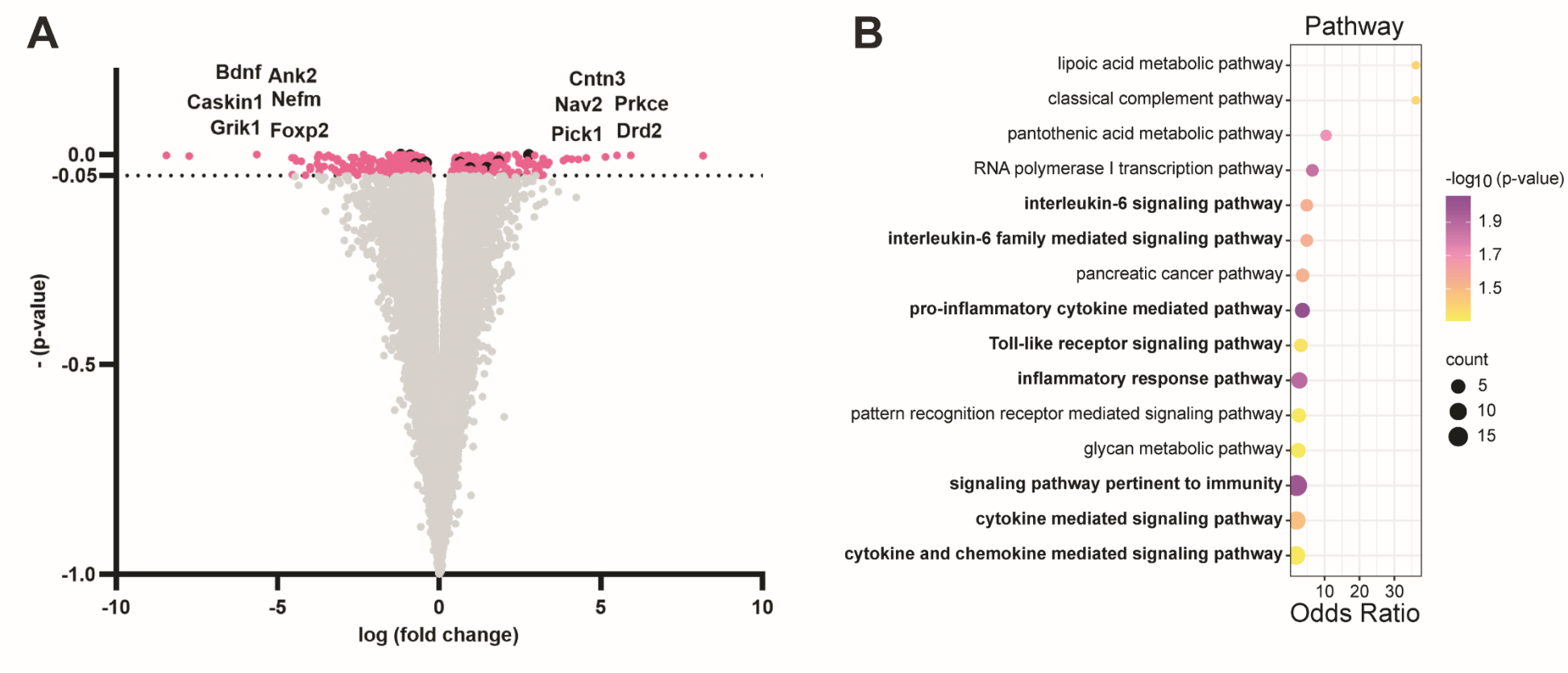

Figure 6: Gene expression profiles of Susceptible versus Intermediate rats. Volcano plot of differentially expressed genes (DEGs) between Susceptible and Intermediate rats using non-adjusted *p* values (**A**). No significant DEGs were identified in the analysis using adjusted *p* values, however, using the non-adjusted *p* value 457 significant ($p < 0.05$) DEGs were identified, indicated in pink. Gene names are indicated for selected genes involved in neuronal functions of interest, with the largest positive fold changes (i.e. upregulated in Susceptible) for the dopamine receptor 2 (*Drd2*) and the largest negative fold changes (i.e. downregulated in Susceptible) for brain-derived neurotrophic factor (*Bdnf*). Biological pathways significantly (uncorrected *p*-value < 0.05) enriched in Susceptible vs. Intermediate rats (**B**) are related to several inflammatory and immune functions (bold text in bubble plot), with the highest Odds Ratio observed for interleukin-6 (IL-6) signalling pathways, indicating these pathways are the most likely to be differentially regulated in the Susceptible compared to Intermediate subgroup of rats.

Supplementary Table 1. Quality report for selected samples

Sample number	Days to <80% BW criterion	Group	RNA Integrity Number (RIN)	BA conc [ng/µl]	i7 Index	Reads (M)
1	/	Resistant	6.5	1.68	TAAGGCGA	34.1
3	/	Resistant	7.2	2.18	TAAGGCGA	88.5
4	4	Susceptible	7.4	1.59	AGGCAGAA	29.0
8	4	Susceptible	6.2	3.04	TCCTGAGC	20.8
9	6	Intermediate	7.7	10.75	GGACTCCT	27.0
11	/	Resistant	6.5	3.02	TAGGCATG	21.6
12	7	Intermediate	9.6	3.74	CTCTCTAC	38.8
15	3	Susceptible	3.4	1.81	CGAGGCTG	29.6
16	3	Susceptible	3.0	1.60	AAGAGGCA	109.9
23	8	Intermediate	3.6	5.97	GTAGAGGA	25.2
26	9	Intermediate	3.8	3.46	GCTCATGA	56.0
27	/	Resistant	4.8	0.51	ATCTCAGG	42.3

Supplementary Information: Definition of Gene Ontology terms

Gene ontology (GO) describes gene functions in three aspects: Molecular Function, Cellular Component, and Biological Process. Molecular function describes the activity of the gene product at molecular level. Cellular component describes the location where the activity occurs in the cell. Biological process represents biological events contributed by molecular processes.

Supplementary Information: Immunohistochemical validation of TRAP expression in striatal projecting mPFC neurons.

Methods

To validate the expression of the EGFPL10a (TRAP) construct, stereotaxic injections were performed as described. Two weeks later, rats (n=2) were euthanized with sodium pentobarbitone (Lethabarb 150mg/kg; Virbac, AU) and transcardially perfused with 200mL 0.9% saline followed by 200mL 4% paraformaldehyde in phosphate buffer. Brains were excised and postfixed in 4% paraformaldehyde in phosphate buffer overnight at 4°C, followed by submersion in 30% sucrose in phosphate buffer for 4 days. Brains were then sectioned at 35µm using a cryostat (CM1860; Leica Biosystems) and collected in a 1:4 series. A series of sections were immunolabeled with chicken anti-GFP (1:1000, Abcam) and guinea pig anti-NeuN (1:1000, Synaptic Systems) primary antibodies overnight at room temperature, followed by 90-minute incubation in Alexa-fluor conjugated secondary antibodies (1:1000, Alexa-fluor 488, Jackson ImmunoResearch; 1:1000, Alexa-fluor 594, Abcam) and 5-minute incubation in DAPI (1:5000, Sigma-Aldrich). Sections were imaged on a widefield microscope (Thunder Imager Live Cell & 3D Assay, Leica Microsystems, Germany).

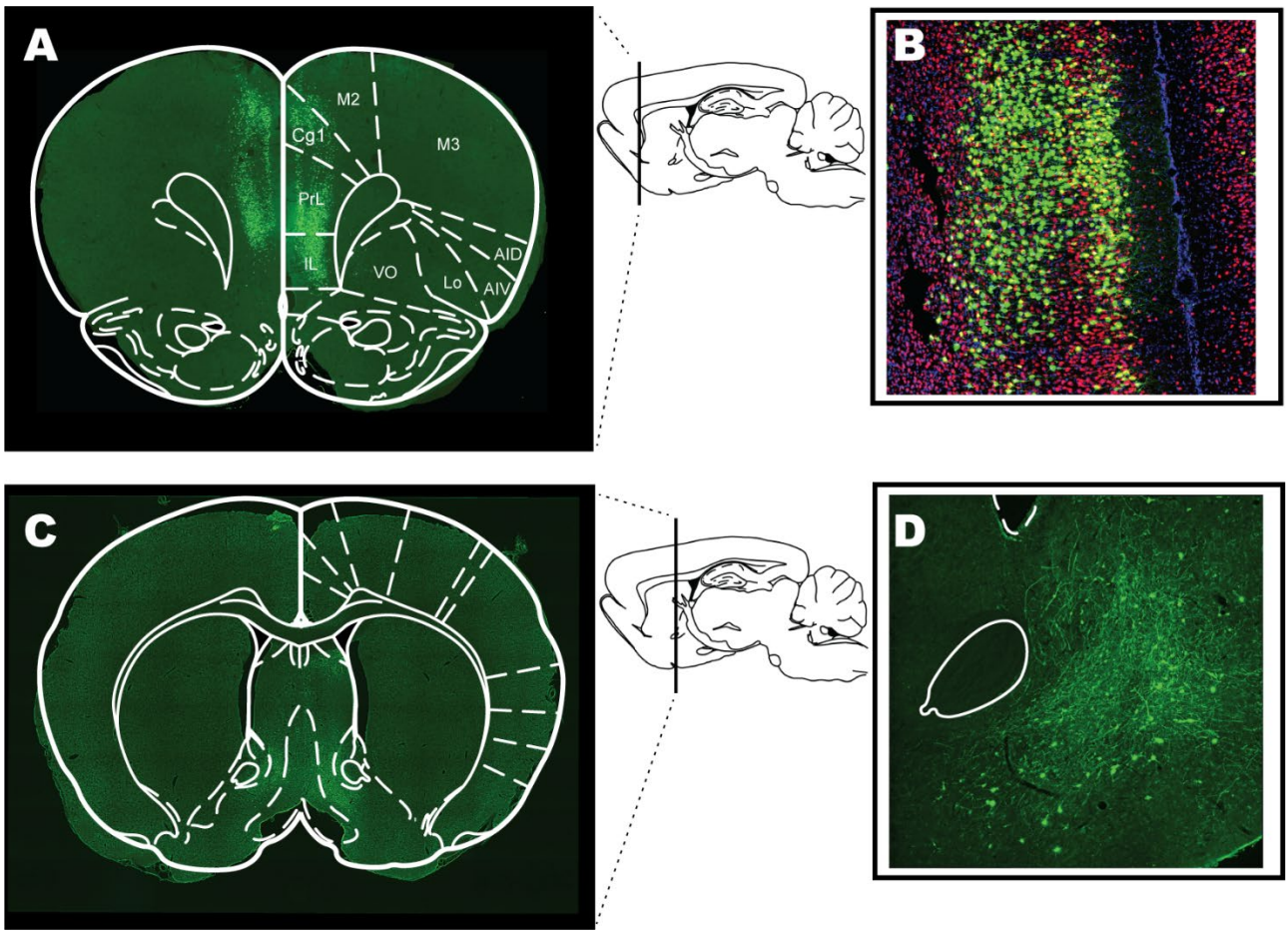

Supplementary Figure 1. EGFPL10a (TRAP) expression is restricted to the medial prefrontal cortex (mPFC). (A) The mPFC region labelled with EFGP collected for RNA sequencing with atlas overlay (Bregma 3.20mm). (B) Micrograph (20X) of the mPFC midline with eGFPL10a (green), NeuN (red) and DAPI (blue) immunofluorescence. (C) The medial AcbSh region confirming terminal staining in the mPFC-AcbSh pathway with atlas overlay (Bregma 0.48mm). (D). Micrograph (20X) of terminal EGFP staining in the AcbSh [markup to orient to the anterior commissure bundle (solid line) and lateral ventricle (dashed line)].

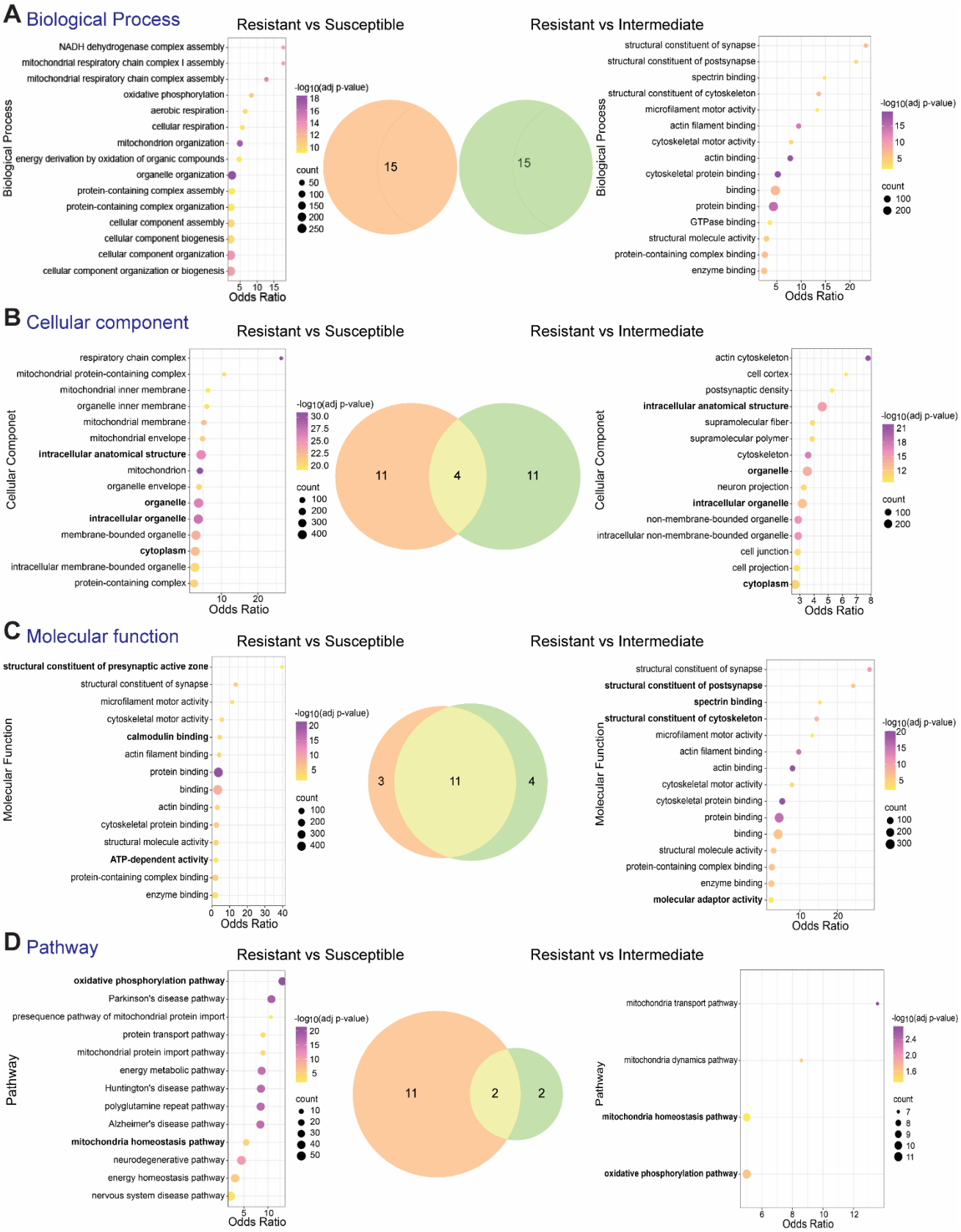
A Biological Process
Resistant vs Susceptible
Resistant vs Intermediate
Biological Process
NADH dehydrogenase complex assembly
mitochondrial respiratory chain complex I assembly
mitochondrial respiratory chain complex assembly
oxidative phosphorylation
aerobic respiration
cellular respiration
mitochondrion organization
energy derivation by oxidation of organic compounds
organelle organization
protein-containing complex assembly
protein-containing complex organization
cellular component assembly
cellular component biogenesis
cellular component organization
cellular component organization or biogenesis
Odds Ratio
-log10(adj p-value)
count
15
15
structural constituent of synapse
structural constituent of postsynapse
spectrin binding
structural constituent of cytoskeleton
microfilament motor activity
actin filament binding
cytoskeletal motor activity
actin binding
cytoskeletal protein binding
binding
protein binding
GTPase binding
structural molecule activity
protein-containing complex binding
enzyme binding
B Cellular component
Cellular Componet
respiratory chain complex
mitochondrial protein-containing complex
mitochondrial inner membrane
organelle inner membrane
mitochondrial membrane
mitochondrial envelope
intracellular anatomical structure
mitochondrion
organelle envelope
organelle
intracellular organelle
membrane-bounded organelle
cytoplasm
intracellular membrane-bounded organelle
protein-containing complex
11
4
11
actin cytoskeleton
cell cortex
postsynaptic density
intracellular anatomical structure
supramolecular fiber
supramolecular polymer
cytoskeleton
organelle
neuron projection
intracellular organelle
non-membrane-bounded organelle
intracellular non-membrane-bounded organelle
cell junction
cell projection
cytoplasm
C Molecular function
Molecular Function
structural constituent of presynaptic active zone
structural constituent of synapse
microfilament motor activity
cytoskeletal motor activity
calmodulin binding
actin filament binding
protein binding
binding
actin binding
cytoskeletal protein binding
structural molecule activity
ATP-dependent activity
protein-containing complex binding
enzyme binding
3
11
4
structural constituent of synapse
structural constituent of postsynapse
spectrin binding
structural constituent of cytoskeleton
microfilament motor activity
actin filament binding
actin binding
cytoskeletal motor activity
cytoskeletal protein binding
protein binding
binding
structural molecule activity
protein-containing complex binding
enzyme binding
molecular adaptor activity
D Pathway
Pathway
oxidative phosphorylation pathway
Parkinson's disease pathway
presequence pathway of mitochondrial protein import
protein transport pathway
mitochondrial protein import pathway
energy metabolic pathway
Huntington's disease pathway
polyglutamine repeat pathway
Alzheimer's disease pathway
mitochondria homeostasis pathway
neurodegenerative pathway
energy homeostasis pathway
nervous system disease pathway
11
2
2
mitochondria transport pathway
mitochondria dynamics pathway
mitochondria homeostasis pathway
oxidative phosphorylation pathway

Supplementary Figure 2. **Gene ontology terms and pathways enriched in differentially expressed genes for Resistant compared to Susceptible or Intermediate subgroups.** The top 15 significantly (corrected *p*-value < 0.05) enriched biological process (**A**), cellular components (**B**), molecular functions (**C**) gene ontology (GO) terms and pathways (**D**) are shown in bubble plots, with Venn diagrams depicting the specific overlap of these GO terms or pathways that were associated with the Susceptible (orange) or Intermediate (green) subgroups compared to Resistant rats. (**A**) The top 15 significant biological process enriched were entirely distinct for the comparisons between Susceptible versus Resistant and Intermediate versus Resistant groups. Differentially expressed genes (DEGs) in the Susceptible subgroup were most significantly associated with mitochondrial function and energy metabolism, whereas DEGs in Intermediate subgroup were mainly associated with cytoskeletal structure and protein interactions. (**B**) Cellular component terms included intracellular anatomical structure, organelle, intracellular organelle and cytoplasm that were common to both subgroups (see bold text term names), whereas mitochondrial structure and function are significantly dysregulated in Susceptible subgroup and cytoskeletal and neuronal structures are associated with the Intermediate subgroup. (**C**) The top 15 molecular function terms largely overlap between the two subgroups (11/15; cytoskeletal dynamics, synaptic function and protein binding), however, pre- and postsynaptic function differed between the comparison groups, whereby presynaptic function was exclusively associated with the Susceptible subgroup and postsynaptic function exclusively within the Intermediate subgroup (see bold terms). (**D**) Pathways associated mitochondrial function (transport, dynamics and homeostasis) are common to both Susceptible and Intermediate subgroups, whereas pathways involved in neurodegenerative diseases (Parkinson's, Huntington's and Alzheimer's Disease) were only seen when comparing the Susceptible subgroup to Resistant rats.

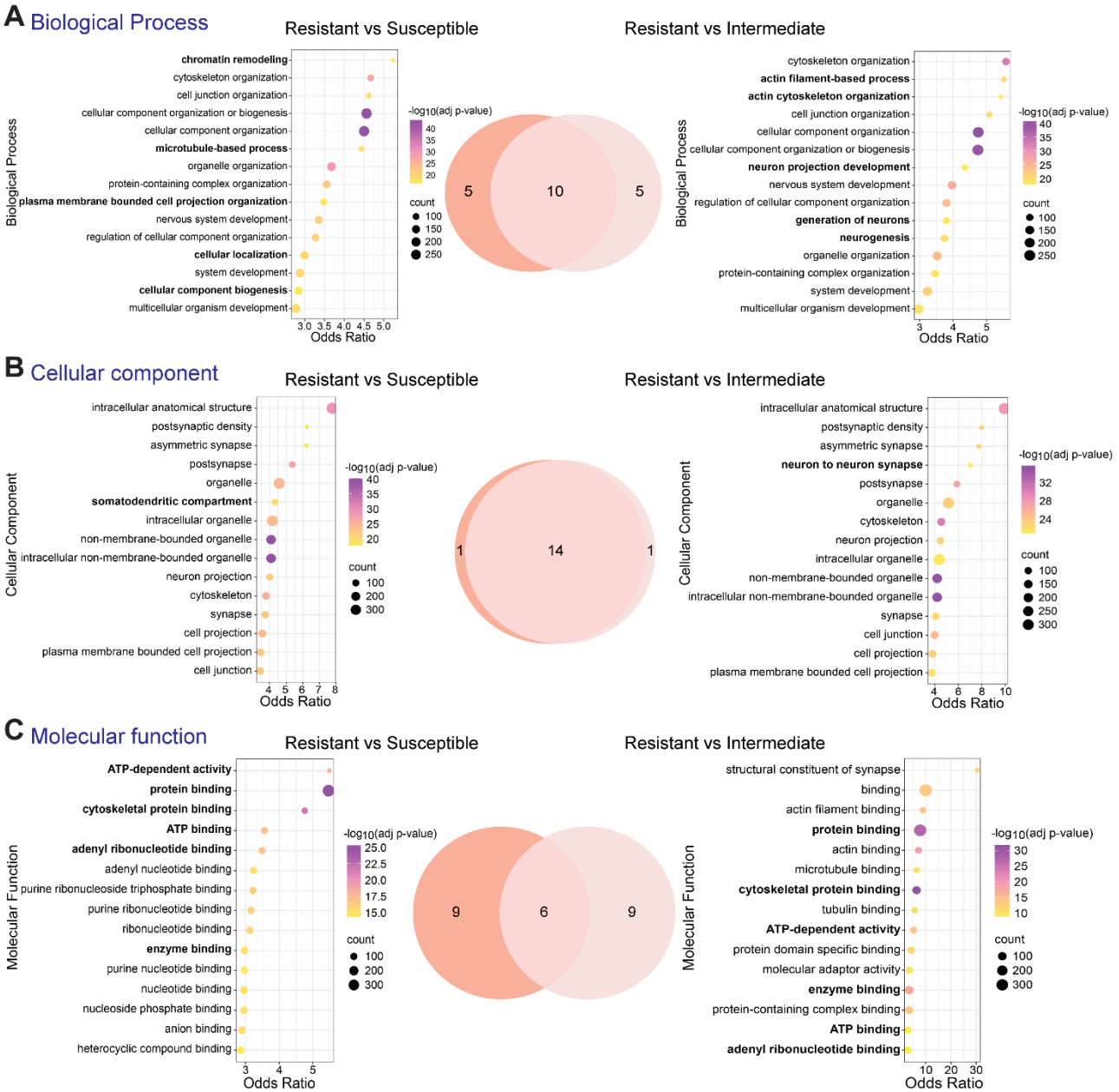
A Biological Process
Resistant vs Susceptible
Resistant vs Intermediate
Biological Process
chromatin remodeling
cytoskeleton organization
cell junction organization
cellular component organization or biogenesis
cellular component organization
microtubule-based process
organelle organization
protein-containing complex organization
plasma membrane bounded cell projection organization
nervous system development
regulation of cellular component organization
cellular localization
system development
cellular component biogenesis
multicellular organism development
Odds Ratio
-log10(adj p-value)
count
5
10
5
neuron projection development
generation of neurons
neurogenesis
B Cellular component
Cellular Component
intracellular anatomical structure
postsynaptic density
asymmetric synapse
postsynapse
organelle
somatodendritic compartment
intracellular organelle
non-membrane-bounded organelle
intracellular non-membrane-bounded organelle
neuron projection
cytoskeleton
synapse
cell projection
plasma membrane bounded cell projection
cell junction
neuron to neuron synapse
1
14
1
C Molecular function
Molecular Function
ATP-dependent activity
protein binding
cytoskeletal protein binding
ATP binding
adenyl ribonucleotide binding
adenyl nucleotide binding
purine ribonucleoside triphosphate binding
purine ribonucleotide binding
ribonucleotide binding
enzyme binding
purine nucleotide binding
nucleotide binding
nucleoside phosphate binding
anion binding
heterocyclic compound binding
structural constituent of synapse
binding
actin filament binding
actin binding
microtubule binding
tubulin binding
protein domain specific binding
molecular adaptor activity
protein-containing complex binding
9
6
9

Supplementary Figure 3. **Gene ontology terms enriched in upregulated differentially expressed genes for Resistant compared to Susceptible or Intermediate subgroups.** The top 15 significantly (corrected *p*-value < 0.05) enriched biological process (**A**), cellular component (**B**), molecular function (**C**) gene ontology (GO) terms are shown in bubble plots, with Venn diagrams depicting the specific overlap of these GO terms that were associated with the Susceptible (orange) or Intermediate (green) subgroups compared to Resistant rats. (**A**) 10 of the top 15 biological processes were enriched for upregulated genes in both Susceptible or Intermediate subgroups, including cellular organization and development, whereas actin cytoskeleton dynamics and neuronal function terms were specific to upregulated genes in the Intermediate subgroup, and the chromatin remodelling and microtubule-based process terms were specific to the Susceptible rats (bold terms). (**B**) Cellular components terms largely overlapped (14/15) involving synaptic functions, cellular organisation and intracellular structures, however the somatodendritic compartment term was specific to the Susceptible subgroup comparison and the neuron to neuron synapse term was specific to the Intermediate subgroup comparison (bold terms). (**C**) Upregulated genes in both subgroups are commonly associated with binding functions (bold), although the specificity of binding terms was a mix of overlapping and distinct.

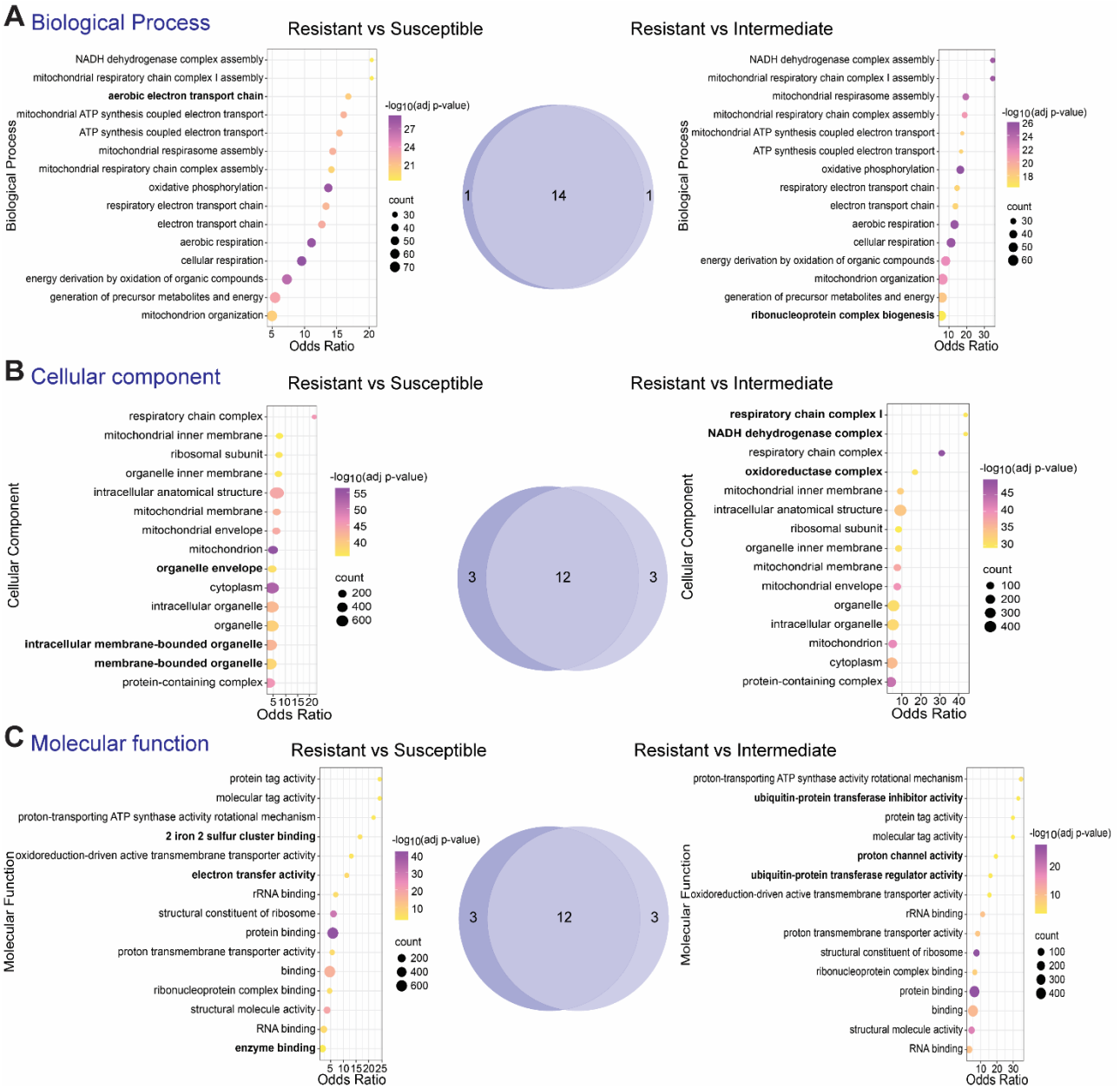

Supplementary Figure 4. Gene ontology terms enriched in downregulated differentially expressed genes for Resistant compared to Susceptible or Intermediate subgroups. Top 15 significantly (corrected *p*-value < 0.05) enriched biological process (**A**), cellular component (**B**), molecular function (**C**) gene ontology (GO) terms are shown in bubble plots, with Venn diagrams depicting the specific overlap of these GO terms that were associated with the Susceptible (orange) or Intermediate (green) subgroups compared to Resistant. (**A**) Biological processes mostly overlap between two subgroup comparisons (14/15), as do (**B**) the cellular components terms (12/15) and (**C**) molecular processes (12/15). The interesting differences between downregulated genes within these comparisons include (**A**) aerobic electron transport chain, (**B**) organelle envelope and (intracellular) membrane-bound organelle, (**C**) 2 iron 2 sulfur cluster binding, electron transfer activity and enzyme binding downregulated in Susceptible; and (**A**) ribonucleoprotein complex biogenesis, (**B**) respiratory chain complex, NADH dehydrogenase complex and oxidoreductase complex, (**C**)

proton channel activity, ubiquitin-protein transferase inhibitor and regulator activity downregulated in Intermediate (see bold text).

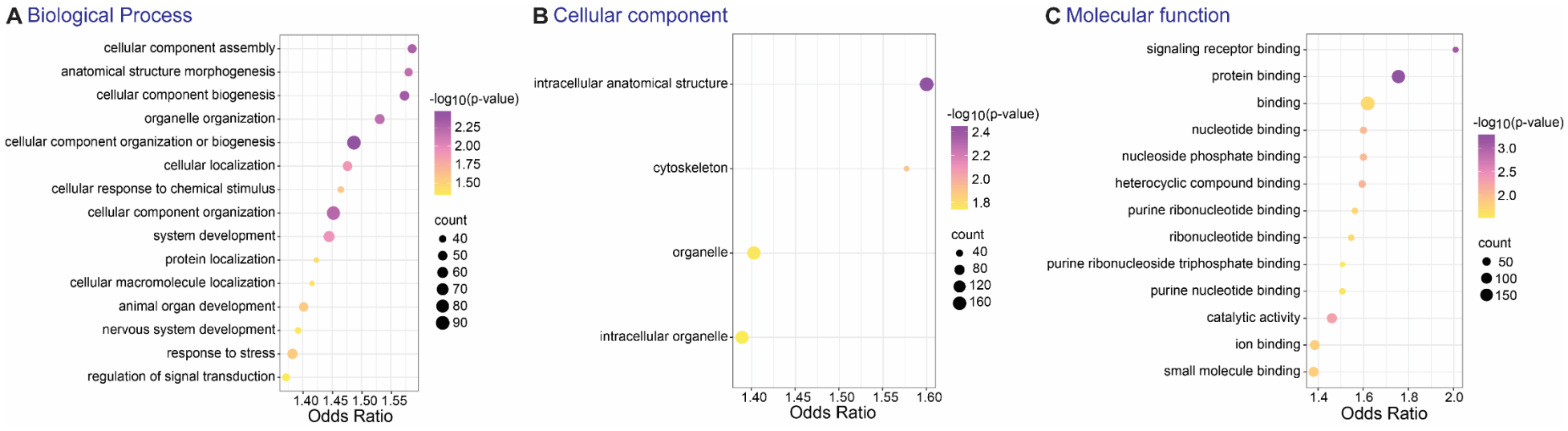

Supplementary Figure 5. Gene ontology terms enriched in genes differentially expressed in Susceptible compared to Intermediate subgroups of ABA rats. Top 15 significantly (*p*-value < 0.05) enriched biological process (**A**), cellular component (**B**), molecular function (**C**) gene ontology (GO) terms are shown in bubble plots. The differentially expressed genes between Susceptible and Intermediate subgroups were mainly associated with intracellular anatomical structure and protein binding functions.